CT Parameters that Influence the Radiation Dose

Hans Dieter Nagel

CONTENTS

H. D. Nagel, PhD
Science and Technology Group, Philips Medical Systems, Roentgenstr. 24, 22335 Hamburg, Germany

The exposure to radiation of patients undergoing computed tomography (CT) examinations is determined by two factors: equipment-related factors, i.e., design of the scanner with respect to dose efficiency, and application-related factors, i.e., the way in which the radiologist or the radiographer makes use of the scanner. In this chapter, the features and parameters influencing patient dose are outlined. First, however, a brief introduction on the dose descriptors applicable to CT is given.

4.1
CT Dose Descriptors

The dose quantities used in projection radiography are not applicable to CT for three reasons:

- First, the dose distribution inside the patient is completely different from that for a conventional radiogram, where the dose decreases continuously from the entrance of the X-ray beam to its exit, with a ratio of between 100 and 1000 to 1. In the case of CT, as a consequence of the scanning procedure that equally irradiates the patient from all directions, the dose is almost equally distributed in the scanning plane. A dose comparison of CT with conventional projection radiography in terms of skin dose therefore does not make any sense.

- Second, the scanning procedure using narrow beams along the longitudinal z-axis of the patient implies that a significant portion of the radiation energy is deposited outside the nominal beam width. This is mainly due to penumbra effects and scattered radiation produced inside the beam.

- Third, the situation with CT–unlike with conventional projection radiography–is further complicated by the circumstances in which the volume to be imaged is not irradiated simultaneously. This often leads to confusion about what the dose from a complete series of, for example, 15 slices might be compared with the dose from a single slice.

As a consequence, dedicated dose quantities that account for these peculiarities are needed: the 'computed tomography dose index (CTDI)', which is a measure of the local dose, and the 'dose–length product (DLP)', representing the integral radiation exposure associated with a CT examination. Fortunately, a bridge exists that enables comparison of CT with radiation exposure from other modalities and sources; this can be achieved by the effective dose (E). So, there are three dose descriptors in all, which everyone dealing with CT should be familiar with.

4.1.1
Computed Tomography Dose Index

The CTDI is the fundamental CT dose descriptor. By making use of this quantity, the first two peculiarities of CT scanning are taken into account: The CTDI [unit: milligray (mGy)] is derived from the dose distribution along a line that is parallel to the axis of rotation for the scanner (= z-axis) and is recorded for a single rotation of the X-ray source. Figure 4.1 illustrates the meaning of this term: CTDI is the equivalent of the dose value inside the irradiated slice (beam) that would result if the absorbed radiation dose profile were entirely concentrated to a rectangular profile of width equal to the nominal beam width $N \cdot h_{col}$, with N being the number of independent (i.e., non-overlapping) slices that are acquired simultaneously. Accordingly, all dose con-
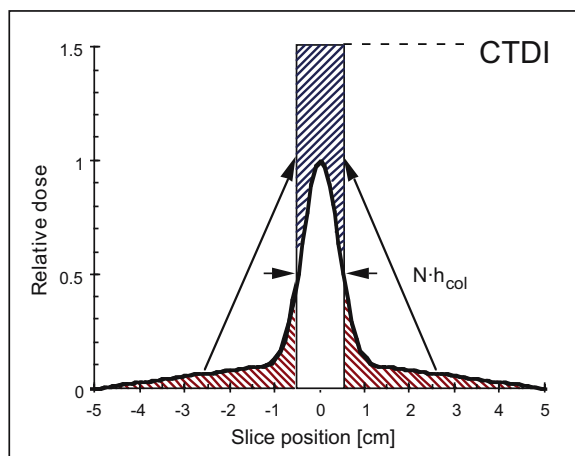
tributions from outside the nominal beam width, i.e., the areas under the tails of the dose profile, are added to the area inside the slice.

The corresponding mathematical definition of CTDI therefore describes the summation of all dose contributions along the z-axis:

$$CTDI = \frac{1}{N \cdot h_{col}} \cdot \int_{-\infty}^{+\infty} D(z) \cdot dz \qquad (4.1)$$

where D(z) is the value of the dose at a given location, z, and $N \cdot h_{col}$ is the nominal value of the total collimation (beam width) that is used for data acquisition. CTDI is therefore equal to the area of the dose profile (the 'dose–profile integral') divided by the nominal beam width. In practice, the dose profile is accumulated in a range of -50 mm to +50 mm relative to the center of the beam, i.e., over a distance of 100 mm.

The relevance of CTDI becomes obvious from the total dose profile of a scan series with, for example, $n = 15$ subsequent rotations (Fig. 4.2). The average level of the total dose profile, which is called 'multiple scan average dose (MSAD)' (Shope 1981), is higher than the peak value of each single dose profile. This increase results from the tails of the single dose profiles for a scan series. Obviously, MSAD and CTDI are exactly equal if the table feed (TF) is equal

Fig. 4.1. Illustration of the term 'Computed Tomography Dose Index (CTDI)': CTDI is the equivalent of the dose value inside the irradiated slice (beam) that would result if the absorbed radiation dose profile were entirely concentrated to a rectangular profile of width equal to the nominal beam width $N \cdot h_{col}$
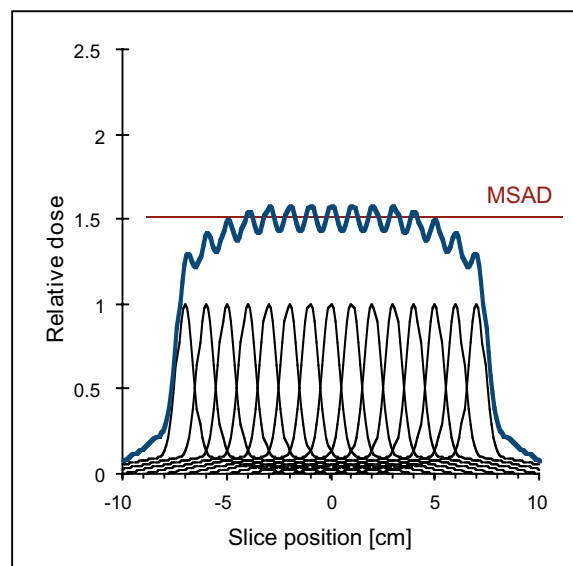

Fig. 4.2. Total dose profile of a scan series with $n=15$ subsequent rotations. The average level of the total dose profile, which is called 'Multiple Scan Average Dose (MSAD)', is equal to the computed tomography dose index (CTDI) if the table feed (TF) is equal to the nominal beam width $N \cdot h_{col}$ (i.e., pitch p = 1)

to the nominal beam width N·h$_{col}$, i.e., if the pitch factor

$$p = \frac{TF}{N \cdot h_{col}} \qquad (4.2)$$

is equal to 1. In general (i.e., if the pitch is not equal to 1, Fig. 4.3), the relationship between CTDI and MSAD is given by

$$MSAD = \frac{1}{p} \cdot CTDI \qquad (4.3)$$

The practical implication of Equation 4.3 is that, in order to obtain the average dose for a scan series, it is not necessary to carry out all the scans. Instead, it is sufficient to obtain the CTDI from a single scan by acquiring the entire dose profile according to Equation 4.1. This is achieved with dose measurements using long, pencil-like detectors, with an active length of 10 cm (Fig. 4.4). These detectors accumulate the dose profile integral (DPI; unit: mGy·cm), i.e., the area under the dose profile shown in Figure 4.1. The CTDI is then obtained according to Equation 4.1 by dividing by the nominal beam width N·h$_{col}$.

In order to obtain estimates of the dose to organs located in the scan range, the CTDI generally refers to standard dosimetry phantoms with patient-like diameters. In the standard measuring procedure for CTDI, which utilizes two cylindrical Perspex

(PMMA) phantoms of different diameter (Fig. 4.4), dose is measured at the center and near the periphery of the phantom (Fig. 4.5). The larger phantom, being 32 cm in diameter, represents the absorption that is typical for the trunk region of adults. The smaller phantom (16 cm in diameter) represents the patient in head examinations. The smaller phantom is also used for dose assessment in pediatric examinations (SHRIMPTON 2000). The dose values thus obtained are denoted as:

$$CTDI_{H,c} \text{ and } CTDI_{H,p} \qquad (4.4a)$$

and

$$CTDI_{B,c} \text{ and } CTDI_{B,p} \qquad (4.4b)$$

with H = head, B = body, c = center, p = periphery.

To make life easier, each pair of CTDI values (central and peripheral) can be combined into a single one named 'weighted CTDI (CTDI$_w$)', which represents the CTDI averaged over the cross section of the pertaining phantom:

$$CTDI_W = \frac{1}{3} \cdot CTDI_{XYZ,c} + \frac{2}{3} \cdot CTDI_{XYZ,p} \qquad (4.5)$$

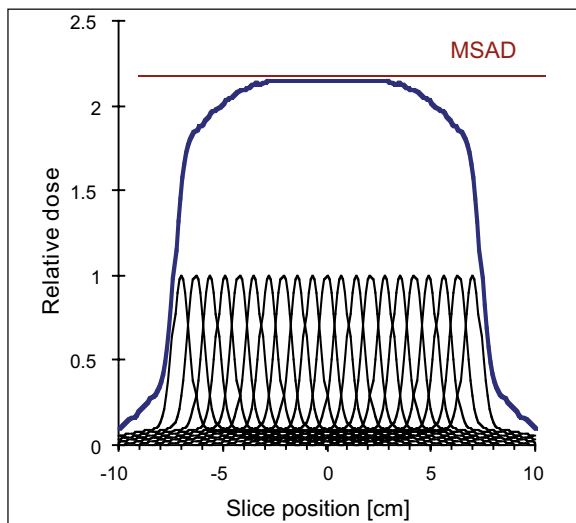where the subscript XYZ stands for either H(ead) or B(ody). In daily practice, CTDI$_w$ is used as one

Fig. 4.3. Total dose profile of a scan series with $n = 15$ subsequent rotations, although scanned with pitch = 0.7. Due to the larger overlap, multiple scan average dose (MSAD) is higher than that in Fig. 4.2 and amounts to computed tomography dose index (CTDI) divided by pitch

Fig. 4.4. Cylindrical standard computed tomography (CT) dosimetry phantoms (16 cm and 32 cm in diameter) made from Perspex for representative measurements of the computed tomography dose index (CTDI) in regions of the head and the trunk, and a pencil-like detector for measurements of the dose-profile integral
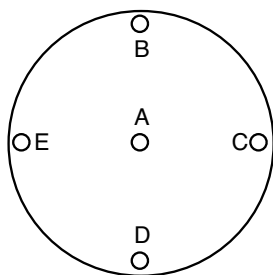
Fig. 4.5. Arrangement of the locations A–E for the determination of the computed tomography dose index (CTDI) in a standard CT dosimetry phantom

of two dose descriptors for dose recommendations ('reference values') that have been introduced by the European Commission (1999a).

If pitch-related effects on the radiation exposure have already been taken into account at the level of local dose (i.e., CTDI), a quantity named 'volume CTDI ($CTDI_{vol}$)' is defined (IEC 2001):

$$CTDI_{vol} = \frac{CTDI_W}{p} \qquad (4.6)$$

So $CTDI_{vol}$ is the pitch-corrected $CTDI_w$. Apart from the integration length, which is limited to 100 mm, $CTDI_{vol}$ is practically identical to MSAD based on $CTDI_w$ (i.e., $MSAD_w$). Since averaging includes both the cross section and the scan length, $CTDI_{vol}$ therefore represents the average dose for a given scan volume. $CTDI_{vol}$ is used as the dose quantity that is displayed at the operator's console of newer scanners. This also holds true even if the display is labeled as '$CTDI_w$' due to faulty definition in the first edition of the particular IEC standard for CT (IEC 1999), or simply as 'CTDI'.

Attention is required if the dose displayed as $CTDI_{vol}$ shall be used for comparison with reference values given in terms of $CTDI_w$. For this purpose, the pitch correction introduced in Equation 4.6 needs to be reversed by multiplying the $CTDI_{vol}$ value by the pitch factor. Care is also required if the $CTDI_{vol}$ displayed is used to assess pediatric radiation exposure: whether head or body CTDI values are displayed depends only on the scan mode (head or body), not on the patient size. Consequently, the dose to children and infants undergoing CT examinations of the trunk region, which for the same scan parameter settings depends on the patient diameter, is currently underestimated with the dose displayed at the operator's console by a factor two to three.

CTDI statements in scanner specification sheets are given for the head phantom as well as for the body phantom and often apply to a current–time product of 100 mAs or 1 mAs. In this case, it must be recognized that a quantity named 'normalized CTDI' is used, which is labeled '$_nCTDI$ (unit: mGy/mAs)' in order to avoid confusion. The normalized CTDI is obtained by dividing the CTDI value by the mAs product Q that was used to measure CTDI:

$$_nCTDI = \frac{CTDI}{Q} \qquad (4.7)$$

It is worthwhile (and indeed necessary) to note that the normalized CTDI is a characteristic quantity for a scanner (dose rate coefficient), which simply represents the capacity of a scanner in terms of output and conveys absolutely nothing about patient dose. Very often it is assumed that scanners with a high value of $_nCTDI$ are more 'dangerous' than other models with lower $_nCTDI$ values. This is not necessarily the case. Reference to patient dose cannot be made unless the normalized CTDI has been multiplied by the tube current–time product Q that is required in order to produce images of diagnostic quality with the type of scanner under consideration. Only after having carried out this step is it possible to decide whether a particular scanner needs more or less dose than another model for a specified type of examination.

4.1.2
Dose–Length Product

The third peculiarity of CT, i.e., the question of what the dose from a complete series of, for example, 15 slices might be compared with that from a single slice, is solved by introducing a dose descriptor named 'dose–length product (DLP; unit: mGy·cm)'. DLP takes both the 'intensity' (represented by the $CTDI_{vol}$) and the extension (represented by the scan length L) of an irradiation into account (Fig. 4.6):

$$DLP = CTDI_{vol} \cdot L \qquad (4.8)$$

So the DLP increases with the number of slices (correctly: with the length of the irradiated body section), while the dose (i.e., $CTDI_{vol}$) remains the same regardless of the number of slices or length. In Figure 4.6, the area of the total dose profile of the scan series represents the DLP. DLP is the equivalent of the dose–area product (DAP) in projection radiography, a quantity that also combines both aspects (intensity and extension) of patient exposure.
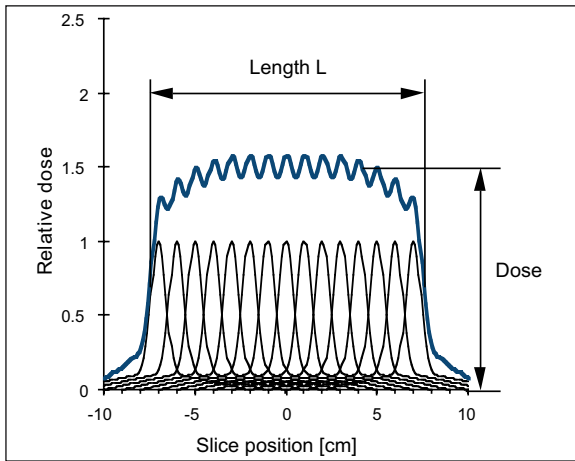
Fig. 4.6. Total dose profile of a scan series with n=15 subsequent rotations. The dose–length product (DLP) is the product of the height (CTDI$_{vol}$) and the width (scan length L) of the total dose profile and is equal to the area under the curve

In sequential scanning, the scan length is determined by the beam width N·h$_{col}$ and the number (n) of table feeds TF):

$$L = n \cdot TF + N \cdot h_{col} \tag{4.9}$$

while in spiral scanning the scan length only depends on the number (n) of rotations and the table feed (TF):

$$L = n \cdot TF = \frac{T}{t_{rot}} \cdot p \cdot N \cdot h_{col} \tag{4.10}$$

where T is the total scan time, t$_{rot}$ is the rotation time, and p is the pitch factor. While in sequential scanning the scan length L is equal to the range from the beginning of the first slice until the end of the last, the (gross) scan length for spiral scanning not only comprises the (net) length of the imaged body section but also includes the additional rotations at the beginning and the end of the scan ('overranging') which are required for data interpolation.

If an examination consists of several sequential scan series or spiral scans, the DLP of the complete examination (DLP$_{exam}$) is the sum of the DLPs of each single series or spiral scan:

$$DLP_{exam} = \sum_i DLP_i \tag{4.11}$$

In daily practice, the DLP is used as the second (and most important) of the two dose descriptors for dose recommendations ('reference values') that have been introduced by the EUROPEAN COMMISSION (1999a).

4.1.3
Effective Dose

CTDI and DLP are CT-specific dose descriptors that do not allow for comparisons with radiation exposures from other sources, e.g., projection radiography, nuclear medicine or natural background radiation. The only common denominator to achieve this goal is the 'effective dose'. With effective dose, the organ doses from a partial irradiation of the body are converted into an equivalent uniform dose to the entire body.

Effective dose E [unit: millisievert (mSv)] according to ICRP 60 (ICRP 1991) is defined as the weighted average of organ dose values H$_T$ for a number of specified organs:

$$E = \sum_i w_i \cdot H_{T,i} \tag{4.12}$$

How much a particular organ contributes to calculation of effective dose depends on its relative sensitivity to radiation-induced effects, as represented by the tissue-weighting factor w$_i$ attributed to the organ:

- 0.20 for gonads
- 0.12 for each of lungs, colon, red bone marrow and stomach wall
- 0.05 for each of breast, urinary bladder, liver, thyroid and esophagus
- 0.01 for each of skeleton and skin
- 0.05 for the 'remainder'

The 'remainder' consists of a group of additional organs and tissues with a lower sensitivity to radiation-induced effects for which the average dose must be used: small intestine, brain, spleen, muscle tissue, adrenals, kidneys, pancreas, thymus and uterus. The sum of all tissue-weighting factors w$_i$ is equal to 1.

Effective dose cannot as such be measured directly in vivo. Measurements in anthropomorphic phantoms with thermo-luminescent dosemeters (TLDs) are very time-consuming and therefore not well suited for daily practice. Effective dose, however, can be assessed in various ways using conversion factors. For coarse estimates, it is sufficient to multiply the DLP with mean conversion factors, depending on which one of three body regions has been scanned and whether that scan was made in head or body scanning mode:

$$E \approx DLP \cdot f_{mean} \tag{4.13}$$

For adults of standard size, the following generic mean conversion factors f_{mean} apply:

1. 0.025 mSv/mGy·cm for the head region
2. 0.060 mSv/mGy·cm for the neck region, scanned in head mode
3. 0.100 mSv/mGy·cm for the neck region, scanned in body mode
4. 0.175 mSv/mGy·cm for the trunk region

Similar factors ('E_{DLP}'), which additionally distinguish between chest, abdomen and pelvis, but do not account for differences in scan mode, are given in report EUR 16262 (European Commission 1999b).

In order to apply Equation 4.13, the DLP or at least the $CTDI_{vol}$ and the (gross) scan length L, from which the DLP can be calculated according to Equation 4.8, must be available. If the scanner is not equipped with a dose display, or if a more detailed assessment of effective dose is desired (e.g., to be more specific for the scanned region of the body, to distinguish between males and females, to assess pediatric doses, or to take differences between scanners into account), dedicated CT dose calculation software should be used. These programs make use of more detailed conversion factors and also allow for calculation of organ doses. Currently, five different programs are in general use. They are available either commercially or as freeware and differ significantly in specifications, performance, and price.

Typical tolerances in effective dose assessment with these programs are in the order of ±20–30%. Similar uncertainties also apply to effective dose assessment with TLD measurements in Alderson phantoms. This should always be borne in mind when comparing doses from different scanners in terms of effective dose. Care is also needed not to mix up effective dose with organ doses, as both are expressed in millisieverts. Nevertheless, effective dose is of great value, e.g., to answer questions raised by patients. For this purpose, the annual natural background radiation, which is between 2 mSv and 3 mSv in most countries, can be used as a scale.

A comprehensive compilation of dose-relevant scanner data and other useful information required for CT dose assessment can be found in a textbook by Nagel et al. (2002). The data given there apply to most of the scanners currently in use, except the most recent. However, data for these new scanners can be found in the CT-Expo software package (Stamm and Nagel 2001), which is based on the data and formalism outlined in this book and is updated regularly.

4.2
Equipment-Related Factors

4.2.1
Beam Filtration

In conventional projection radiography, beam filtration is a well-known means to reduce those portions of the radiation spectrum with no or little contribution to image formation. In the early years of CT history, beam filtration was comparatively large in order to compensate for beam-hardening artifacts. Filters made from 0.5 mm of copper, with filtering properties equivalent to approximately 18 mm of aluminum (quality equivalent filtration, Nagel 1986), were not unusual at that time. The present generation of scanners typically employs a beam filtration for the X-ray tube assembly of between 1 mm and 3 mm aluminum and an additional filtration (flat filter) of 0.1 mm copper, giving a total beam filtration of between 5 mm and 6 mm aluminum.

Apart from this, there are a number of older and also newer scanners that operate with an added filtration of approximately 0.2 mm copper, resulting in a total beam filtration of between 8 mm and 9 mm aluminum, and sometimes even more (currently up to 12 mm aluminum quality-equivalent filtration). Likewise, there are also scanners that employ less filtration. Consequently, the normalized dose values for these scanners ($_nCTDI$ in terms of mGy/mAs) differ significantly. Very often these lower or higher values are misunderstood as being an indicator that the equipment is more or less dose efficient compared with other scanners. This might not necessarily be the case in reality.

Apart from dose, the consequences on image quality arising from the beam hardening and beam attenuating properties of filtration have also to be considered (Nagel 1989). The use of additional filtration impairs primary contrast and increases noise due to reduced beam intensity per mAs, as experienced by the detectors. Without compensating for these adverse effects (e.g., by increasing tube current–time product), the contrast-to-noise ratio (CNR), which affects the detectability of small or low-contrast details, is reduced. Unpublished studies by the author show that, in order to maintain the CNR (i.e., for constant image quality), the net reduction in terms of effective dose achieved by increasing the standard beam filtration (1 mm Al + 0.1 mm Cu = 4.5 mm Al quality equivalent) by 0.2 mm Cu

amounts to not more than 10%, even in favorable situations (soft tissue imaging, Fig. 4.7). Conversely, the same added filtration leads to higher patient doses (up to 15%) in examinations with administration of contrast agents (iodine). At the same time, tube loading must be increased by 20% in order to compensate for reduced beam intensity.

Newer surveys on CT practice (GALANSKI et al. 2001) revealed that scanners of comparable age, but with largely differing beam filtration, are operated at almost similar dose levels. Similar results in terms of dose efficiency have been found in comparative tests on scanners with differing beam filtration conducted by ImPACT (2004). Contrary to projection radiography, which operates at comparatively lower tube potentials, beam filtration plays only a minor role in CT, where higher tube potentials are applied. A return to increased beam filtration–as sometimes recommended or practiced–is less advantageous than expected and should only be made if sufficient X-ray tube loading capacity is available or if other important aspects exist (e.g., improved performance of reconstruction filters).
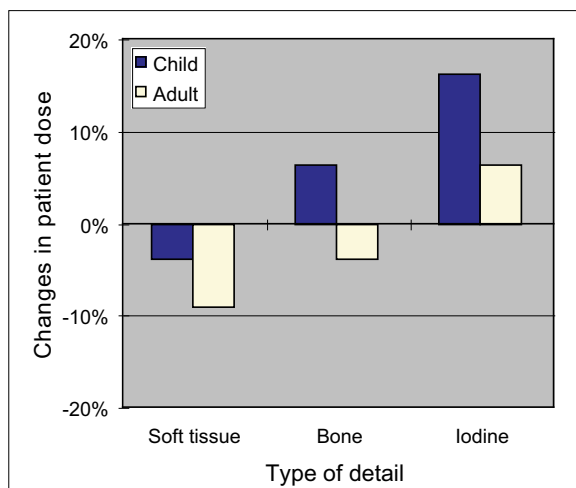

Fig. 4.7. Changes in patient dose due to increased beam filtration at constant contrast-to-noise ratio for different types of detail. Standard filtration: 1 mm Al + 0.1 mm Cu (= 4.5 mm Al quality equivalent); added filtration: 0.2 mm Cu (= 7 mm Al quality equivalent)

4.2.2
Beam Shaper

Most scanners are equipped with a dedicated filter device, named 'beam shaper' or 'bow-tie filter', that modifies the spatial distribution of radiation emitted within the fan beam. The purpose of this kind of filter (which is characterized by increasing thickness toward its outer edges) is to adapt the beam intensity to match the reduced attenuation of objects in the outer portions of the fan beam. Dynamic range requirements for the detector system can thus be reduced. Simultaneously, beam-hardening effects are also less likely.

In order to provide attenuating properties that are almost tissue equivalent, beam shapers should be made from materials containing only elements with a low atomic number Z. However, this is not always the case in practice. Beam shapers preferentially affect the dose in the outer portions of an object, thereby reducing the peripheral $CTDI_p$ values. But, as the dose at the center is mainly caused by scattered radiation from the periphery of the object, the central $CTDI_c$ value is also somewhat reduced. The ratio of dose at the periphery to that at the center therefore decreases, making the dose distribution inside an object more homogeneous and so improving the uniformity of noise in the image. Contrary to the flat filter, the beam shaper has a much greater impact on the dose properties of a scanner.

The beam shapers found in practice not only differ by the material from which they are made. They also differ by their shape, thus producing more or less compensation. A prominent example is the beam shaper of the Elscint CT Twin, which was modified in 1998 to produce more compensation. In addition, different types of beam shapers can be selected on some scanners, depending on the nature and diameter of the object (e.g., for head and body scanning mode).

4.2.3
Beam Collimation

The beam collimation for defining the thickness of the slice to be imaged is made in the first instance close to the X-ray source (primary collimation). The shape of the dose profile is determined by the aperture of the collimator, its distance from the focal spot, and the size and shape (i.e., the intensity distribution) of the focal spot. Due to the narrow width of collimation, penumbral effects occur. These effects become more and more pronounced as collimation is further narrowed.

In addition, there is a secondary collimation close to the detector ('post-patient collimation') that primarily serves to remove scattered radiation. On some single-slice and dual-slice scanners, this secondary

collimation is further narrowed in order to improve the shape of the slice profile ('restrictive post-patient collimation', Fig. 4.8a,b). For multi-slice scanners with more than two detector rows, the primary collimation must necessarily be made wider than N_{times} the selected slice collimation in order to avoid (or at least to reduce) penumbral effects in the outer portions of the detector array (Fig. 4.8c). In both cases, the dose profile is wider than the slice profile or the nominal beam width, and the patient is exposed to a larger extent ('overbeaming'), as becomes obvious from normalized CTDI values that increase with reduced beam width.

Overbeaming can be expressed by a single parameter, the 'overbeaming parameter' dz, which is equal to the combined width of the portion of the dose profile not used for detection (Fig. 4.8c). Overbeaming itself, i.e., the percentage increase in CTDI due to the unused portion of the dose profile, is then given by

$$\Delta CTDI_{rel} = \frac{dz}{N \cdot h_{col}} \cdot 100 \qquad (4.14)$$

The overbeaming parameter dz typically amounts to 1 mm for single- and dual-slice scanners that employ restrictive post-patient collimation, and to 3 mm for multi-slice scanners with $N=4$ and more slices that are acquired simultaneously, although this may vary depending on the type of scanner. For narrow beam-width settings, the increase in dose that results from overbeaming can be 100% and more.

In practice, overbeaming is no real issue for single- and dual-slice scanners, as the limited coverage restricts the use of narrow beam width to a few examinations with a short scan range (e.g., inner ear). With multi-slice scanners, however, overbeaming effects have to be taken seriously, as multi-slice computed tomography (MSCT) technology aims to provide improved resolution along the z-axis, which requires reduced slice collimation. Overbeaming, i.e., the increase in CTDI that results from beamwidth settings that are typical for each type of scanner, is shown in Figure 4.9 for a number of scanners from different manufacturers. As indicated by the trend line, overbeaming is most pronounced with quad-slice scanners and is diminished with an increasing beam width $N \cdot h_{col}$ provided by scanners with more slices (NAGEL 2005).

4.2.4
Detector Array

In contrast to single-slice scanners, multi-slice scanners are equipped with a detector array that consists of more than a single row of detectors. Gas detectors or fourth-generation stationary detector rings are no longer compatible with multi-slice requirements. Consequently, only third-generation detector arcs with solid-state detectors have remained. In general, solid-state detectors are more dose efficient than gas
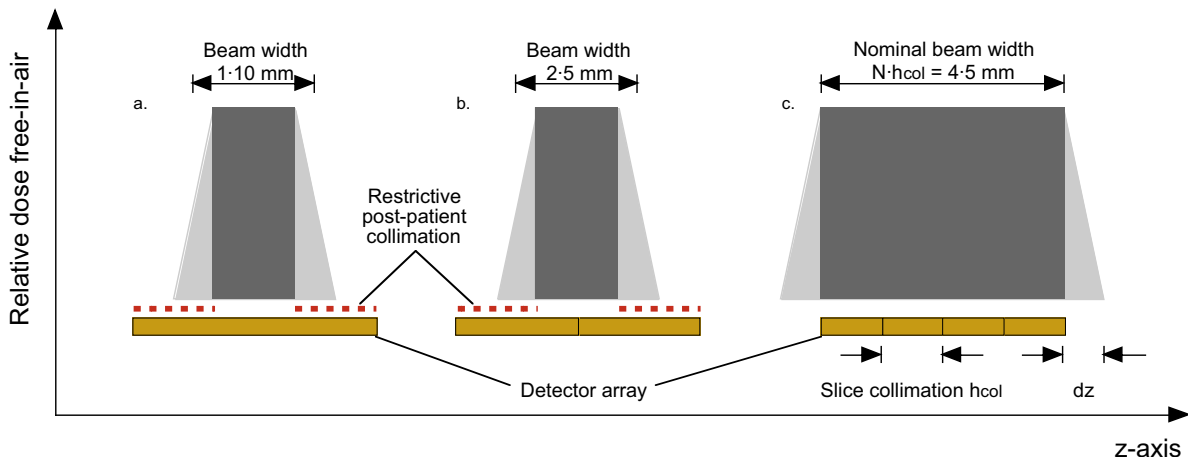

Fig. 4.8a–c. Dose profiles free-in-air with umbra (*dark gray*) and penumbra (*light gray*) portions for a single-slice scanner (**a**), a dual-slice scanner (**b**), and a quad-slice scanner (**c**). With single- and dual-slice scanners, the width of the active detector rows is sufficient to capture the entire dose profile, penumbra included (except for some scanners that employ restrictive post-patient collimation). For scanners with four and more slices acquired simultaneously, penumbra is excluded from detection in order to serve all detector channels equally well. The combined width of the penumbra triangles at both sides is characterized by the overbeaming parameter dz
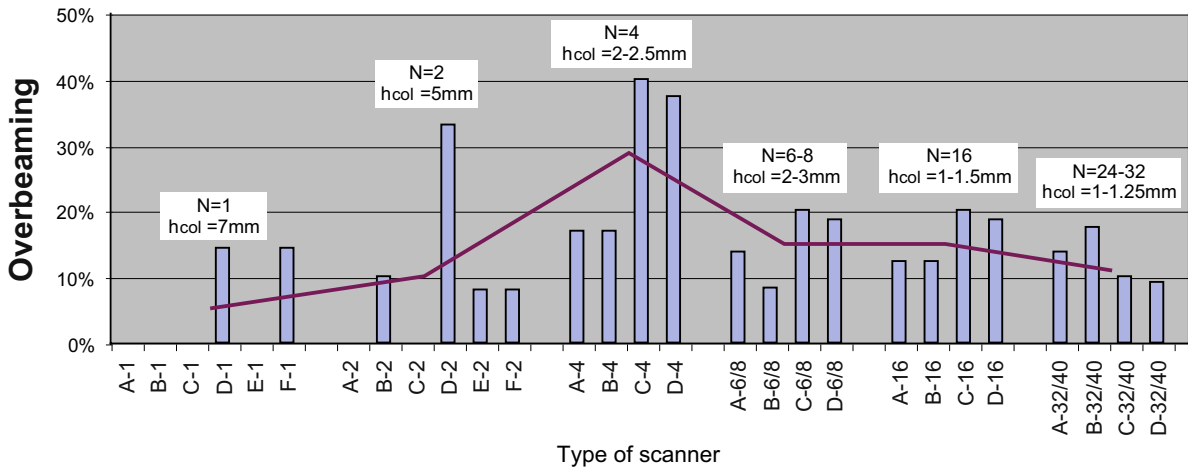
Fig. 4.9. Overbeaming, i.e., the percentage increase in the computed tomography dose index (CTDI), for single-slice ($N=1$), dual-slice ($N=2$), quad-slice ($N=4$), 6 to 8-slice ($N=6–8$), 16-slice ($N=16$) and 32 to 40-slice ($N=32–40$) scanners from different manufacturers (A–F) for the slice collimations h_{col} typically employed. The *red trend line* indicates that overbeaming is most pronounced with quad-slice scanners in practice and is diminished with an increasing beam width $N·h_{col}$

detectors (VAN DER HAAR et al. 1998), but require additional means to suppress scattered radiation (anti-scatter-grids) that inevitably cause a certain loss of primary radiation, too.

The single detectors in a multi-row, solid-state detector array are separated by narrow strips ('septa') which are not sensitive to radiation and therefore do not contribute to detector signal. Due to the large number of additional strips, these inactive zones result in minor or major geometrical losses, depending on the design of the detector array. In addition, further losses occur due to a decrease in sensitivity at the edges of each row that results from cutting the scintillator crystal. In contrast to a single-row detector array, the width of which can be larger than the maximum slice thickness (Fig. 4.10), the edges of the rows in a multi-row detector array are located inside the beam. Due to both these effects–separating strips and decreased sensitivity–the net efficiency of a solid-state detector array, which is typically 85% for single-slice scanners, is further decreased, typically to 70%.

When 4-slice scanners were introduced in 1998, very different detector designs were used (Fig. 4.11), with variations in the number of rows (between 8 and 34) and the smallest detector size (between 0.5 mm and 1.25 mm). The large number of rows (much larger than the number of slices that can be acquired simultaneously) was necessary to enable the use of different slice collimations (between 4×0.5 mm and 4×8 mm). Slice collimations wider than the detector size were achieved by electronically combining sev-
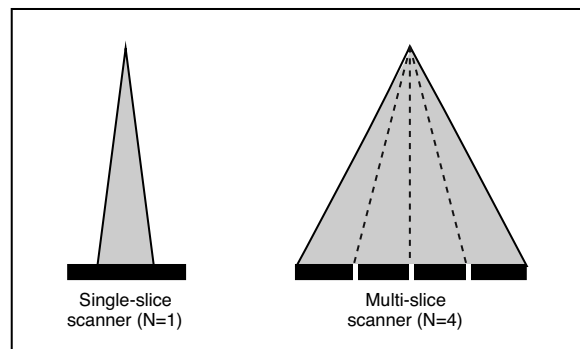

Fig. 4.10. A multi-slice computed tomography (MSCT) scanner, with simultaneous scanning of four slices, compared with a conventional single-slice scanner. Due to the additional septa between the detector rows, the geometric efficiency of MSCT detector arrays is comparatively lower by 10–20%

eral adjacent detector rows [e.g., 4×1.25 mm = 5 mm (GE) or 1+1.5+2.5 = 5 mm (Philips/Siemens)]. Each detector design had its specific advantages and drawbacks: Toshiba's hybrid arrangement offered the largest coverage (32 mm) and the acquisition of four sub-millimeter slices, but had the largest number of septa (1 per mm) and the smallest detector size (0.5 mm). The progressive design, commonly used by Philips and Siemens, had the smallest number of septa (0.35 per mm), but was restricted to two sub-millimeter slices only. GE's matrix arrangement was a compromise (0.75 per mm) that, however, facilitated the next technology step toward eight simultaneously acquired slices with the same detector array.

All 16-slice scanners introduced in 2001 now made use of the same hybrid design, with 16 smaller central detectors, accompanied by a number of larger detectors at both sides (Fig. 4.12). Apart from the number of detector rows (between 24 and 40) and array width (between 20 mm and 32 mm), there were differences in the size of the detectors (between 0.5 mm and 1.5 mm), and each manufacturer claimed his solution to be the best. As in real life, there are a number of conflicting needs (spatial resolution, dose efficiency, coverage) that must be met, especially with respect to cardiac imaging where scan times below 20 s (one breathhold) are mandatory. Consequently, any design that emphasized only one of these criteria was definitely not the best compromise. Due to the increased number of septa [from 0.6 per mm (4-slice) to 1.1 per mm (16-slice) on average], the geometric efficiency of 16-slice detector arrays is somewhat lower.

In the latest generation of 64-slice scanners, matrix arrangements that allow for simultaneous acquisition of 64 sub-millimeter slices are employed by the majority of manufacturers (Fig. 4.13). By electronically combining several adjacent rows, thicker slices can also be acquired, but this results in a reduced number of slices (e.g., 32×1.25 mm, 16×2.5 mm, etc.). Once again, the number of septa was increased (to 1.6 per mm on average), resulting in an additional loss in geometric efficiency.

The hybrid detector design exclusively used by Siemens for its Sensation 64 scanner is uncommon, insofar as the number of simultaneous slices claimed by the manufacturer (64) is much larger than the number of rows (32×0.6 mm or 24×1.2 mm). The claim is based on a special acquisition mode that employs two alternating focal spot positions to simultaneously produce 64 data sets per rotation with 50% overlap in order to achieve a somewhat
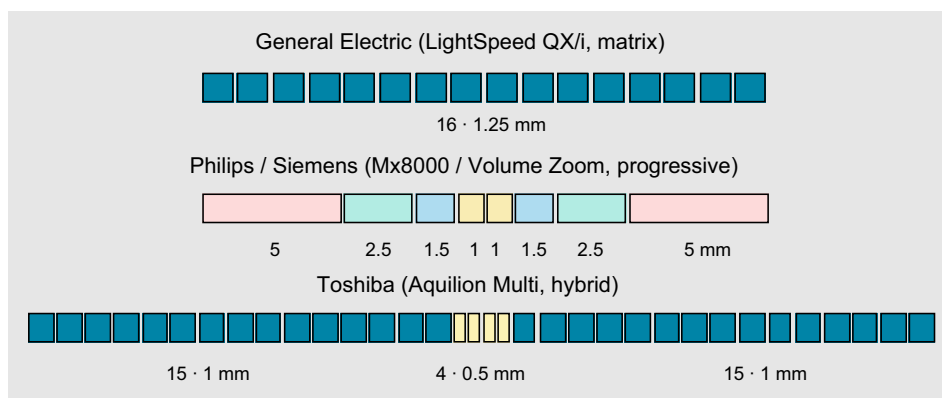

Fig. 4.11. Detector arrangement of four-slice scanners with significant differences in design (number of rows, detector size, array width). Most are optimized for simultaneous acquisition of four slices
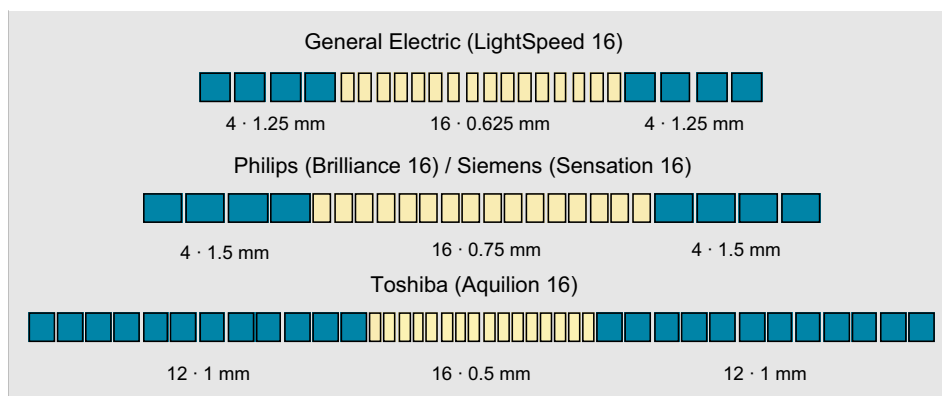

Fig. 4.12. Detector arrangement of 16-slice scanners, all of which employ a hybrid design, but with differences in the number of rows, detector size, and array width
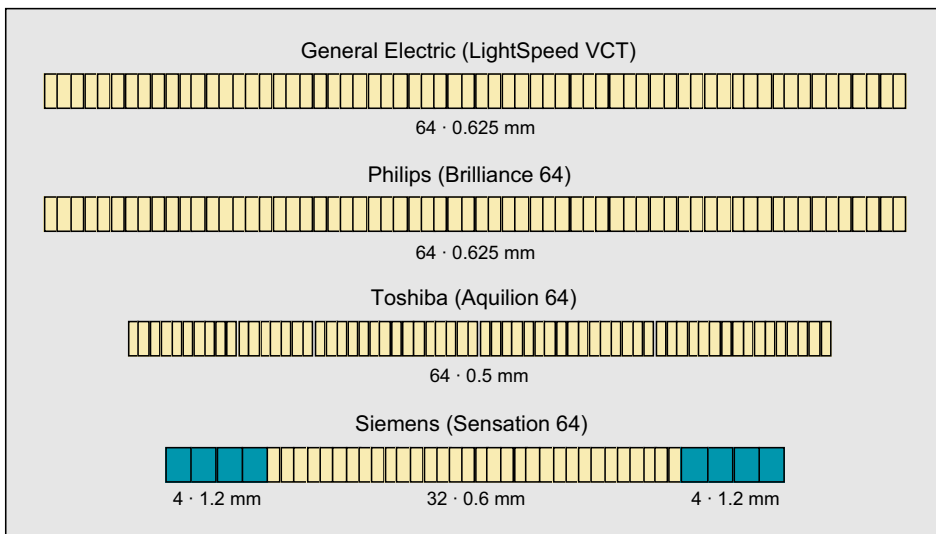
Fig. 4.13. Detector arrangement of 64-slice scanners, most of which employ a matrix design with 64 rows of uniform size. The Siemens design refers to a 32-slice scanner that makes use of a particular acquisition mode (alternating focal spot) with 64 overlapping (i.e. non-independent) slices

improved spatial resolution in the z-direction. With respect to all other important features (collimation, coverage, overbeaming effects, etc.), however, this model behaves as a 32-slice scanner in submillimeter mode and a 24-slice scanner in all other modes at maximum. In addition, the thickness of the smallest slice that can be reconstructed (relevant for partial volume effects) is at least equal to the smallest slice collimation, i.e., 0.6 mm (FLOHR et al. 2004), not lower.

4.2.5
Data Acquisition System

The data acquisition system (DAS) serves to collect the detector signals, to convert them into digital information and to transfer the data to the image reconstruction system. The number of DAS channels, not the number of detector rows, is the decisive parameter that limits the number of independent slices that can be acquired simultaneously. Consequently, the term 'MDCT (multi-detector-row CT)' is somewhat misleading, as has recently happened to the term 'MSCT (multi-slice CT)', too. Thus, 'multi-channel CT (MCCT)' would be the most unequivocal notation.

With the advent of 16-slice scanners at the latest, the spatial requirements of an increased number of detector rows and the exorbitantly increased data rate no longer allow use of traditional circuit

Fig. 4.14. The spatial requirements of an increased number of detector rows and the exorbitantly increased data rate necessitated the development of data acquisition systems with tiny application-specific integrated circuits (ASICs) that replaced the traditional circuit boards (courtesy: Philips Medical Systems)

boards. Instead, application-specific integrated circuits (ASICs) have been developed, with significantly reduced dimensions (Fig. 4.14) and drastically increased data transfer capabilities. As these ASICs operate with reduced electronic noise, they are advantageous with respect to the dose efficiency of the detector assembly. This is demonstrated in Figure 4.15 where the dose that is necessary to obtain images of equal image noise at equal slice thickness was reduced by 25% with the introduction of this advanced DAS chip (VLASSENBROEK 2004).
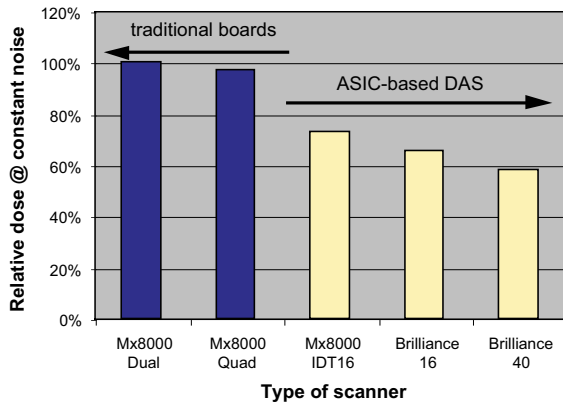
Fig. 4.15. As a side effect, the lower electronic noise of ASIC-based data acquisition systems introduced with 16-slice scanners allows for a 25% dose reduction at constant noise (beam width for all scanners: N·h$_{col}$ = 10 mm)

4.2.6
Spiral Interpolation

Data acquisition in spiral scanning mode requires an additional interpolation step to obtain axial slices. The interpolation scheme of single-slice scanners employs two data points for each projection angle only, thus producing a bell-shaped slice profile. Depending on whether only true data (360° linear interpolation (LI), Fig. 4.16a) or also virtual data (180° LI, Fig. 4.16b) are used, the width of the slice profile is significantly broadened with increasing pitch (Fig. 4.18a). The relative noise, however, remains independent from pitch and amounts to 83% (360° LI) and 117% (180° LI) compared with sequential scanning.

Most multi-slice scanners make use of a different interpolation scheme with more than two data points ('z-filtering', TAGUCHI and ARADATE 1998). Depending on the slice thickness h$_{rec}$ to be reconstructed, interpolation is made using all data points that are located inside the pre-selected filter width (FW; = h$_{rec}$, Fig. 4.17). Contrary to single-slice scanners, the width of the slice profile thus remains unaffected from changes in pitch settings of up to p = 2 (Fig. 4.18b).

However, as the number of data points inside FW is reduced, the noise will increase with pitch unless corrective actions are taken. This can be accomplished by adjusting the (electrical) tube current I$_{el}$ proportional to the change in pitch p. This adjustment is automatically made for all MSCT scanners from Elscint, Philips and Siemens, thereby using a different mAs notation (Q$_{eff}$) named 'effective mAs'

or 'mAs per slice', which is different from the traditional electric mAs product Q$_{el}$:

$$Q_{eff} = \frac{I_{el} \cdot t_{rot}}{p} = \frac{Q_{el}}{p} \qquad (4.15)$$

As a result, pitch has no longer any influence on slice profile width, image noise and average dose (CTDI$_{vol}$) if Q$_{eff}$ is held constant. This does not hold for MSCT scanners manufactured by General Electric and Toshiba, which do not automatically correct the tube current for pitch and do not use effective mAs notation.

4.2.7
Adaptive Filtration

Adaptive filtration (AF) is a dedicated data processing technique for projections that are subject to strong attenuation. Without AF, images, e.g., from the pelvis region, often exhibit inhomogeneous noise patterns due to 'photon starvation' (Fig. 4.19, left). The noise statistics of these projections are improved by making use of additional data close to the position of the reconstructed slice, i.e., by increasing the FW at the level of image reconstruction. However, as indicated in Figure 4.20, this is made only for those projections that suffer from excessive attenuation. Thus, the spatial resolution in the z-direction is only slightly impaired. As a result, images processed with AF show a reduced and more homogeneous noise pattern (Fig. 4.19, right). This can be used either to improve the image quality or to lower the dose settings.

4.2.8
Overranging

'Overranging' is the increase in DLP due to the additional rotations at the beginning and at the end of a spiral scan required for data interpolation to reconstruct the first and the last slice of the imaged body region. With single-slice scanners, the theory requires that Δn = 1 additional rotation is usually made in total (KALENDER 2000). For multi-slice scanners, the situation is much less obvious, as will be seen from the results presented below.

Overranging effects can be expressed in terms of both the additional number Δn of rotations and the increase ΔL in scan length. ΔL depends primarily on two factors: the beam width N·h$_{col}$ and the pitch fac-
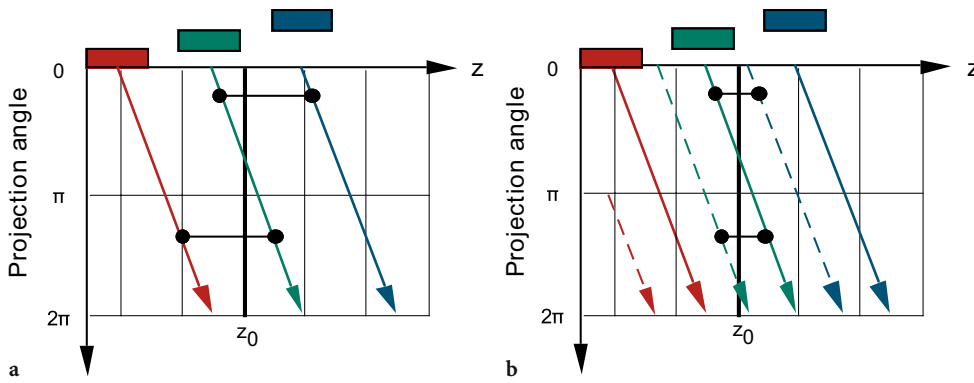
Fig. 4.16a,b. The most common interpolation schemes for single-slice scanners are either 360° LI (**a**) or 180° LI (**b**). Both schemes employ two data points closest to the position z_0 of the reconstructed slice for each projection angle. Making use of the virtual (*complementary*) data (*dashed lines*), a shorter interpolation distance is achieved with 180° LI, resulting in a narrower slice profile
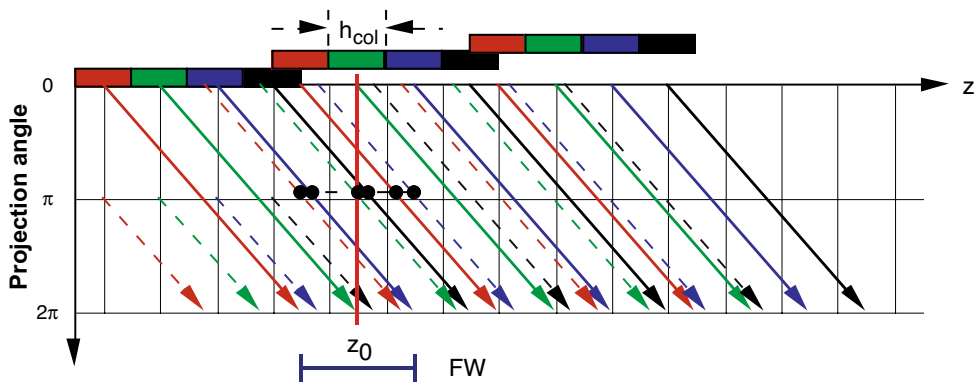

Fig. 4.17. Most multi-slice computed tomography (MSCT) makes use of a filtered multi-point data interpolation scheme (z-filtering). All data points (true and virtual) lying inside a pre-selected filter width (FW) contribute to the slice reconstructed at position z_0, with slice thickness $h_{rec} = FW$. In this example, the interpolation scheme for a 4-slice scanner at pitch 0.875 is shown (FW = 2·h_{col})
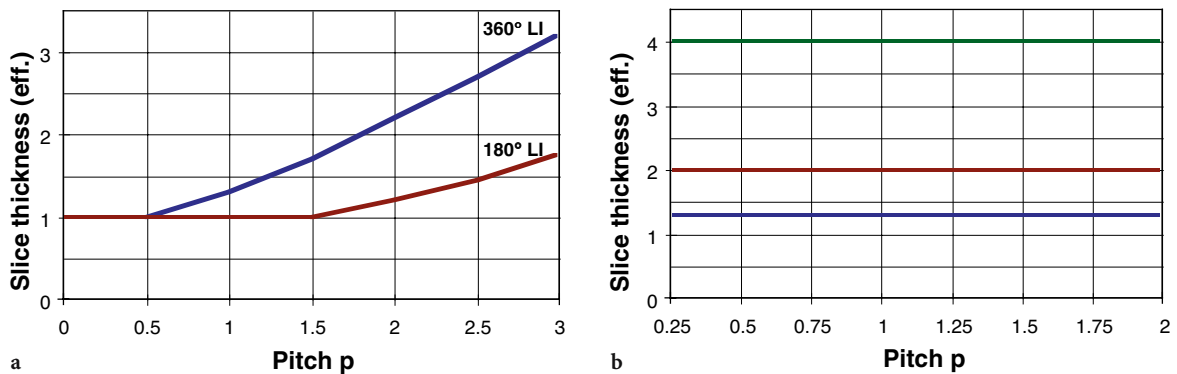

Fig. 4.18a,b. With single-slice scanner, two-point data interpolation results in a significant broadening of the effective slice thickness with increasing pitch, depending on the selected interpolation scheme (**a**). The multi-point data interpolation used for most multi-slice scanners ensures a constant effective slice thickness regardless of the pitch setting that depends only on the selected filter width and holds up to p = 2 (**b**)
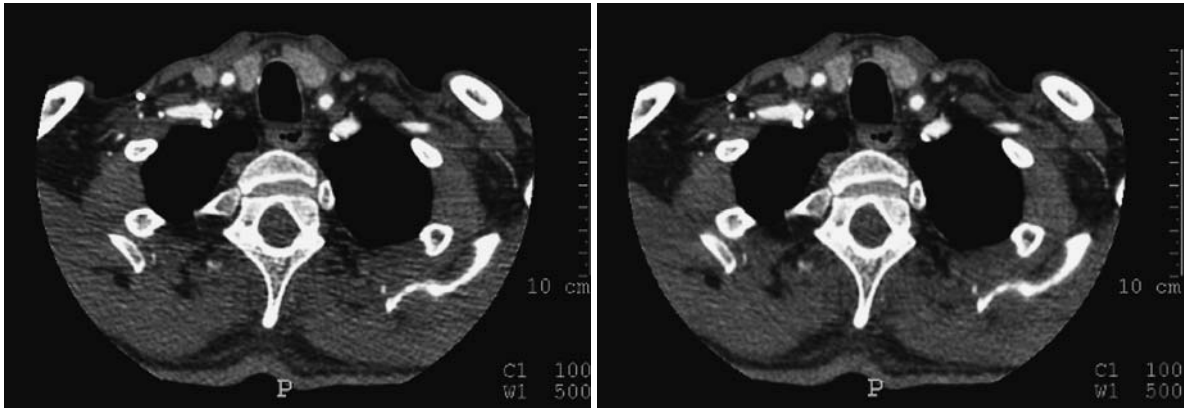
Fig. 4.19. Projections suffering from excessive attenuation result in images with unisotropic noise patterns (*left*); images processed with adaptive filtration show a reduced and more homogeneous noise pattern (*right*)
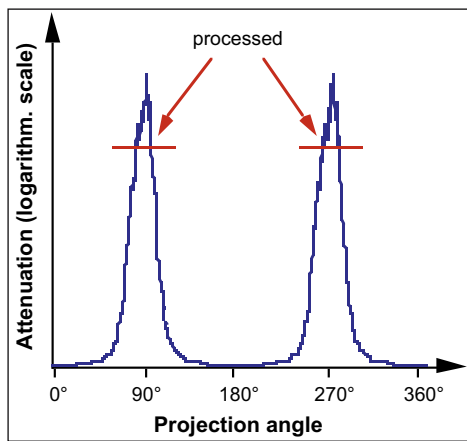

Fig. 4.20. Adaptive filtration affects only those projections where the attenuation exceeds a pre-selected level

tor p. This can be fairly well described by a linear relationship (NAGEL 2005):

$$\Delta L = (m_{OR} \cdot p + b_{OR}) \cdot N \cdot h_{col} \qquad (4.16)$$

While single-slice scanners behave as expected from theory, the characteristics of typical MSCT scanners differ markedly. The number Δn of additional rotations (Fig. 4.21a) is strongly pitch dependent, while the normalized elongation of the scan range, $\Delta L/N \cdot h_{col}$, is almost independent of pitch (Fig. 4.21b) and amounts to approximately 1.5, i.e., ΔL is typically 1.5 times the total beam width $N \cdot h_{col}$. For most single-slice scanners, the overranging parameters m_{OR} and b_{OR} are equal to 2 and –1, respectively. For the majority of MSCT scanners, typical values for m_{OR} and b_{OR} are 1 and 0.5, respectively.

The implications of overranging effects for the radiation exposure to the patient, i.e., the DLP, depend not only on ΔL, but also on the length L_{net} of the imaged body region. The percentage increase in DLP is given by

$$\Delta DLP_{rel} = \frac{\Delta L}{L_{net}} \cdot 100 \qquad (4.17)$$

and will be largest if ΔL is large and L_{net} is small.

The extent of overranging is shown in Figure 4.22 for a representative selection of single and multi-slice scanners from different manufacturers for typical scan parameter settings and a typical scan length of 20 cm. Overranging effects are normally almost negligible for single-slice and the majority of dual- and quad-slice scanners. Contrary to overbeaming, overranging becomes larger with an increasing number of slices acquired simultaneously due to the enlarged beam width. Even greater values might occur for beam widths larger than the typical ones assumed here and scan ranges shorter than 20 cm.

4.2.9
Devices for Automatic Dose Control

Newer scanners are equipped with means that automatically adapt the mAs settings to the individual size and shape of the patient. As this matter is discussed in detail in Chapter 6, only a brief overview shall be given here.

Automatic dose control systems offer up to four different functionalities, that can be used either alone or in combination:
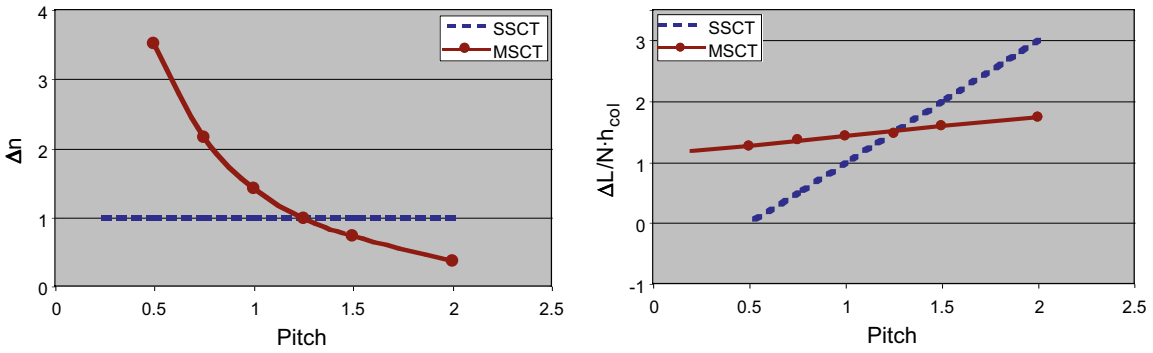
Fig. 4.21. While single-slice computed tomography scanners (SSCTs) usually require only one additional rotation Δn in spiral scanning mode, multi-slice computed tomography scanners (MSCTs) show a pronounced pitch dependence. Conversely, the normalized elongation of the scan range, $\Delta L / N \cdot h_{col}$, is almost constant for most MSCT scanners, but increases linearly with pitch for SSCT scanners
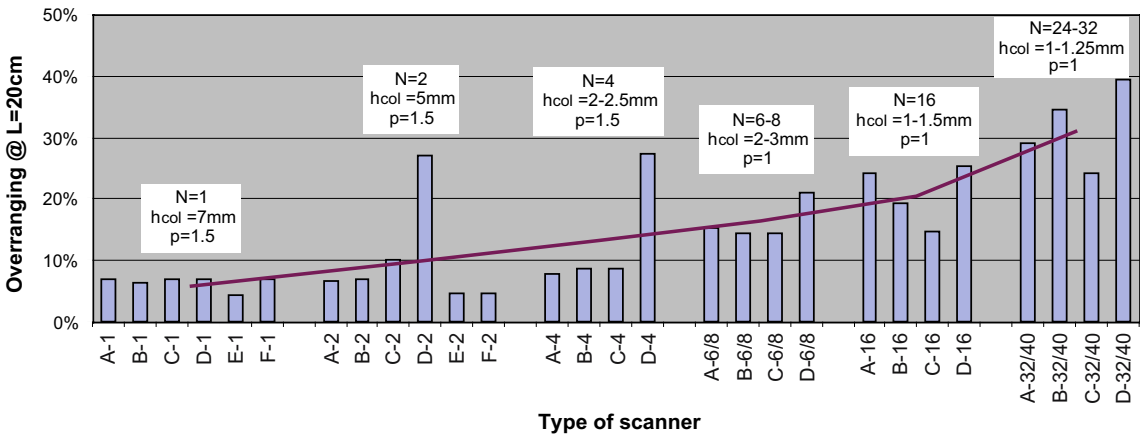

Fig. 4.22. Overranging, i.e., the percentage increase in dose–length product (DLP), for single-slice ($n = 1$), dual-slice ($n = 2$), quad-slice ($n = 4$), 6 to 8-slice ($n = 6$–8), 16-slice ($n = 16$) and 32 to 40-slice ($n = 32$–40) scanners from different manufacturers (A–F) for a scan length L of 20 cm and the slice collimations and pitch settings typically employed. The *red trend line* indicates that overranging becomes more pronounced with scanners that allow for a wider beam width $N \cdot h_{col}$

- Automatic exposure control (AEC, Fig. 4.23), which accounts for the average attenuation of the patient's body region that is to be scanned. Information on the patient's attenuation properties is derived from the scan projection radiogram (SPR) usually recorded prior to the scan for planning purposes.
- Longitudinal dose modulation (LDM, Fig. 4.24), which is a refinement of AEC by adapting the mAs settings locally, i.e., slice-by-slice or rotation by rotation.
- Angular dose modulation (ADM, Fig. 4.25), another refinement of AEC that adapts the tube current to the varying attenuation at different projection angles. Information on the patient's attenuation properties is derived either from two SPR or in real-time from the preceding rotation.
- Temporal dose modulation (TDM, Fig. 4.26), which reduces the tube current in cardiac CT (or other ECG-gated CT examinations) during those phases of the cardiac cycle that are not suited for image reconstruction due to excessive object motion.

The common denominator of these functionalities is that the user no longer needs to select his parameter settings with respect to the 'worst case',
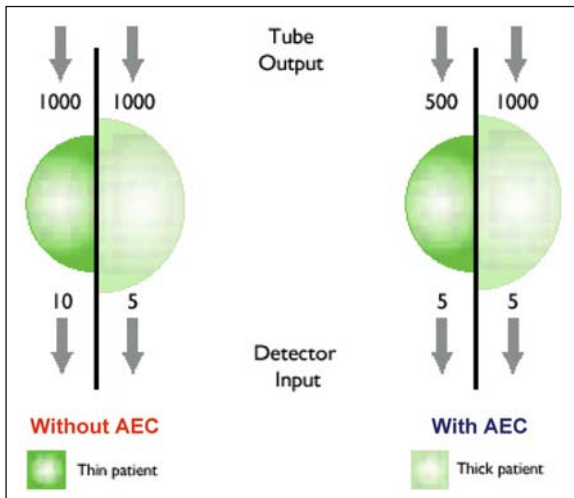
Fig. 4.23. Automatic exposure control (AEC) accounts for the average attenuation of the patient's body region that is to be scanned. For slim patients, mAs is reduced to a level that ensures constant image quality
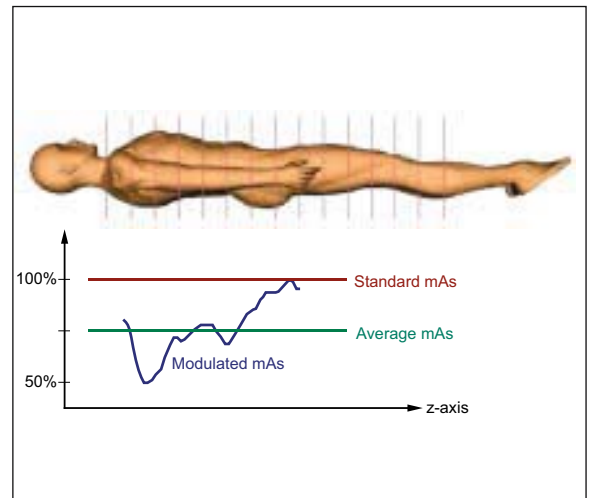
Fig. 4.24. Longitudinal dose modulation (LDM) is a refinement of AEC that adapts the mAs settings slice-by-slice or rotation by rotation. Those parts of the scan range with reduced attenuation will be less exposed
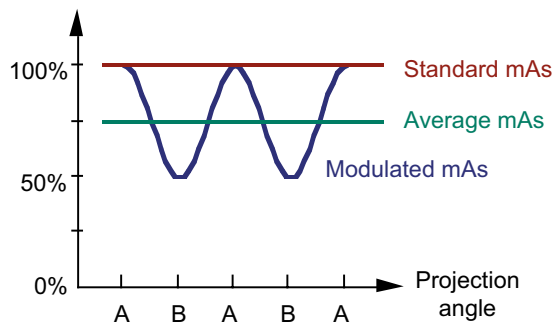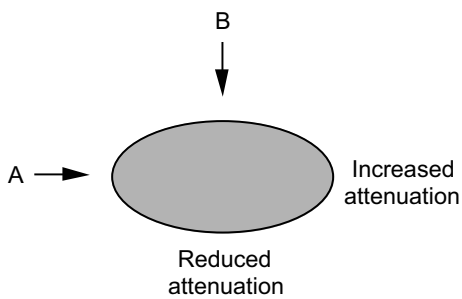
Fig. 4.25. Angular dose modulation (ADM) is an other refinement of AEC that adapts the tube current to the varying attenuation at different projection angles. Those projections with reduced attenuation will be less exposed
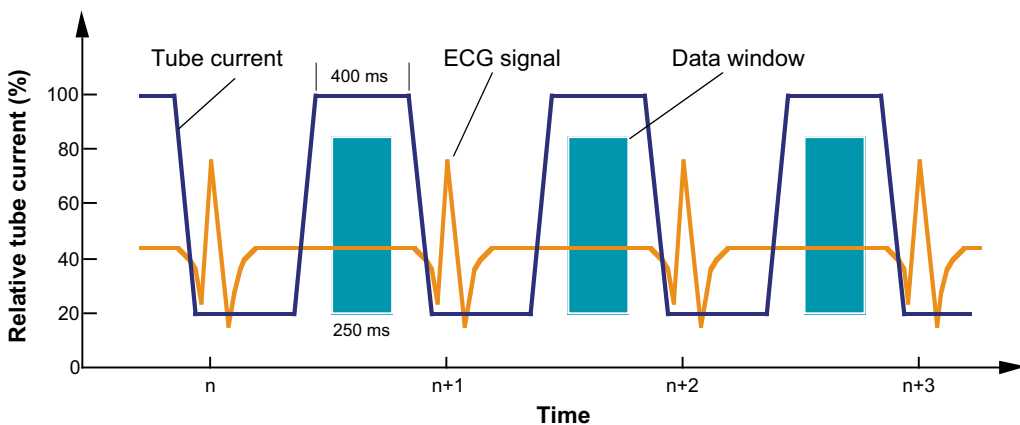
Fig. 4.26. In cardiac computed tomography (CT; or other ECG-gated CT examinations), temporal dose modulation (TDM) reduces the tube current during those phases of the cardiac cycle that are not suited for image reconstruction due to excessive object motion

i.e., obese patients, the part of the scan range with the highest attenuation (e.g., shoulder in chest exams), the projection with the highest attenuation (lateral), etc. Consequently, a significant dose reduction from the application of these devices can be expected.

All major CT manufacturers now offer some or all of these functionalities with their latest scanners. A comprehensive report on the current status of automatic dose control systems has been published by ImPACT (2005). However, there are significant differences in how these devices operate and perform. At present, some of these systems are not sufficiently user-friendly and make adjustments in a way that seems to be theoretically sound, but does not comply with other, more comprehensive aspects of image quality. Some of these shortcomings will be discussed in the following section.
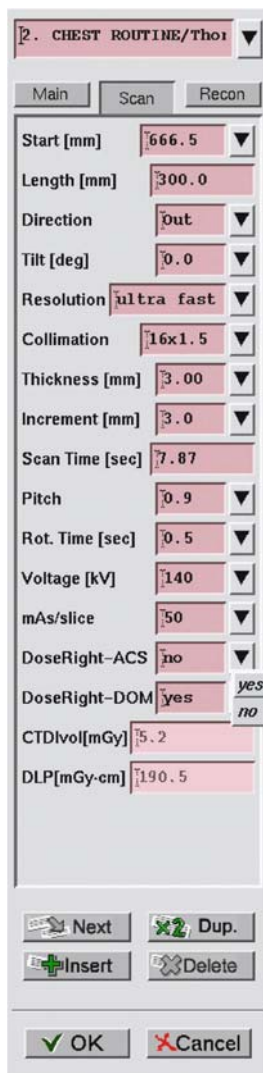

Fig. 4.27. Scan protocol window of a Philips Mx8000 IDT scanner with dose display (CTDI$_{vol}$ and DLP per scan series) at the bottom

4.2.10
Dose Display

Newer scanners must be equipped with a dose display. At present, only the display of CTDI$_{vol}$ is mandatory (IEC 2001). However, many scanners already also show the DLP, either just per scan series or both per scan series and per exam. An example with display of CTDI$_{vol}$ and DLP per scan series is shown in Figure 4.27.

With the dose display, dose is not saved per se, but feedback is provided that may help to achieve this goal, e.g., by comparison of the displayed dose values with dose recommendations. In addition, changes in scan parameter settings and their implications for patient exposure are made immediately obvious. Thus, the dose display can be used for purposes of dose optimization. Finally, CTDI$_{vol}$ can be used as a fair estimate for the dose to organs that are entirely located in the scan range.

The interpretation of the dose values displayed at the scanner's console needs special attention in the following situations:

- Many dose recommendations are given in terms of weighted CTDI (CTDI$_w$); in order to allow for comparisons, the pitch correction involved in CTDI$_{vol}$ must be reverted by multiplying CTDI$_{vol}$ by the pitch factor.
- Until now, the dose values for examinations carried out in body scanning mode have always been based on body-CTDI regardless of patient size. In pediatric CT examinations, the displayed figures should be multiplied by 2 for children and by 3 for infants in order to give a realistic estimate of patient dose.

4.3
Application-Related Factors

Although the scanner design is of some importance, surveys on CT practice have regularly shown that the way that the scanner is used has the largest impact on the doses applied in a CT examination. The application-related factors on which patient exposure depends can be grouped into:

- Scan parameters, i.e., those factors that directly determine the local dose level (CTDI$_{vol}$) and that are often pre-installed or recommended by the manufacturer (e.g., in application guides)

- Examination parameter, i.e., those factors that–in combination with CTDI$_{vol}$–determine the integral exposure (i.e., DLP) and depend on the preferences of the user
- Reconstruction and viewing parameters, which implicitly influence the dose settings

First, however, the principal inter-dependence between dose settings and image quality shall be outlined

4.3.1
Brooks' Formula

As in conventional projection radiography, aspects of dose and image quality are linked. For CT, BROOKS and DiCHIRO (1976) have formulated the correlation between these two opposed quantities:

$$D \propto \frac{B}{\sigma^2 \cdot a^2 \cdot b \cdot h} \text{ with } B = \exp^{-\mu \cdot d} \qquad (4.18)$$

where

    D = patient dose
    B = attenuation factor of the object
    μ = mean attenuation coefficient of the object
    d = diameter of the object
    σ = standard deviation of CT numbers (noise)
    a = sample increment
    b = sample width
    h = slice thickness

This fundamental equation–commonly known as the 'Brooks' formula'–describes what happens with respect to patient dose if one of the parameters is changed while image noise remains constant:
- Dose must be doubled if slice thickness is cut by half
- Dose must be doubled if object diameter increases by 4 cm
- An eightfold increase in dose is required if spatial resolution is doubled (by cutting sample width and sample increment by half)

In this context, the term 'dose' is applicable to each of the dose quantities that are appropriate for CT. Dose and noise are inversely related to each other in such a way that a fourfold increase in dose is required if noise is to be cut by half.

It should be noted, however, that the Brooks' formula is incomplete, in that image quality is only considered in terms of quantum noise and spatial resolution. Other important influences, such as contrast, electronic noise and artifacts, are not taken into account and will therefore modify optimization strategies under particular circumstances.

4.3.2
Scan Parameters

4.3.2.1
Tube Current–Time Product (Q)

As in conventional radiology, a linear relationship exists between the tube current–time product and dose; i.e., all dose quantities will change by the same amount as the applied mAs. The mAs product Q for a single sequential scan is obtained by multiplying the tube current I and exposure time t; in spiral scanning mode, Q is the product of the tube current I and rotation time t$_{rot}$ .This should not be mixed up with the total mAs product of the scan which is the product of tube current I and (total) scan time T.

The consequences on image quality resulting from variations in the tube current–time product are relatively simple to understand. The only aspect of image quality so affected is image noise, which is–as indicated in Equation 4.18–inversely proportional to the square root of dose (i.e., mAs).

The tube current–time product is often used as a surrogate for the patient dose (i.e., CTDI). However, this is highly misleading, as the normalized CTDI values and thus the dose that results for the same mAs setting can vary by up to a factor of six between different scanners. So it makes absolutely no sense to communicate dose information or recommendations on the basis of mAs. Instead, only CTDI$_{vol}$ (and DLP) should be used for this purpose.

With the advent of multi-slice scanners, additional confusion arose due to the introduction of a different, pitch-corrected mAs notation ('effective mAs' or 'mAs per slice', Eq. 4.15) by Elscint, Philips and Siemens. As most multi-slice scanners make use of a multi-point spiral interpolation scheme as outlined in section 4.2.6, effective mAs is the most appropriate notation for MSCT. Nevertheless, General Electric and Toshiba still prefer the traditional electrical mAs notation, which further makes it difficult to compare mAs settings among different scanners. This particularly holds for cardiac CT where very low pitch settings are used.

Recommendation:

The settings for the tube current–time product should be adapted to the characteristics of the scanner, the size of the patient (see section 4.3.2.5), and the dose requirements of each type of examination. Examinations with high inherent contrast, such as for chest or skeleton, that are characterized by viewing with wide window settings, can regularly be conducted at significantly reduced mAs settings.

4.3.2.2
Tube Potential (U)

When the tube potential is increased, both the tube output and the penetrating power of the beam are improved, while image contrast is adversely affected. In conventional projection radiography, increased tube potentials are applied in order to ensure short exposure times for obese patients, to equalize large differences in object transmission (e.g., during chest examinations) or to reduce patient dose. In the latter case, automatic exposure control devices guarantees that the improved penetrating power of the beam is exclusively for the benefit of the patient.

In CT, increased tube voltages are used preferentially for improvements in tube loading and image quality. Contrary to the case for mAs, the consequences of variations in kV cannot easily be assessed. The relationship between dose and tube potential U is not linear, but rather of an exponential nature which varies according to the specific circumstances. The intensity of the radiation beam at the detector array, for example, varies with U to the power of 3.5. If the tube potential is increased, e.g., from 120 kV to 140 kV, the electrical signal obtained from the detectors therefore changes by a factor 1.7 (Fig. 4.28).

The decrease in primary contrast which normally results from this action is largely overcompensated by the associated decrease in noise, i.e., the higher the tube potential, the better the CNR (except for the application of iodine as contrast agent). The only reason why this analysis generally holds true is the absence of any kind of automatic exposure control devices in the majority of scanners which might prevent unnecessary increases in the detector signal. This clearly demonstrates that dose is not reduced by applying higher kilovolt settings, but merely increased as long as mAs settings are not changed: weighted CTDI and effective dose increase with U to the power of 2.5 (Fig. 4.28), which means that both are increased by approximately 50% if kilovolt settings are changed from 120 kV to 140 kV.

Therefore the question of whether and when it might be reasonable to deviate from the 120-kV setting usually applied is justified. As can be seen from Figure 4.29, this depends on the attenuation characteristics of the detail that is diagnostically relevant. The figures are given in terms of contrast-to-noise ratio squared (CNR^2) at constant patient dose; this notation allows direct conversion of the percentage differences into dose differences. For soft tissue contrast (e.g., differences in tissue density), higher tube potentials perform slightly better than lower ones, but the differences are quite small. The opposite holds true for bone contrast (i.e., bone versus tissue). For iodine contrast, however, there is a strong dependence on tube potential that is much in favor of lower kilovolt settings. Thus, 80 kV instead of 120 kV would allow reduction of the patient dose
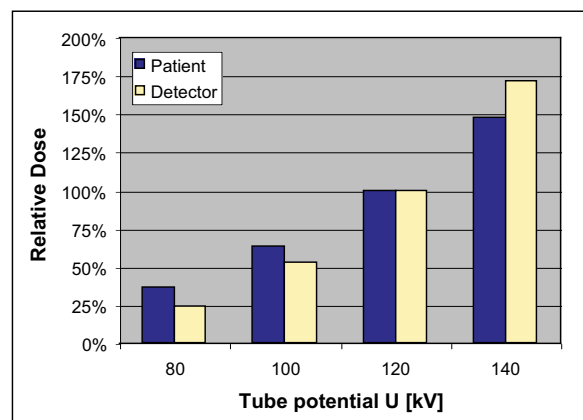

Fig. 4.28. Voltage dependence of patient dose ($CTDI_w$) and detector signal (reference: 120 kV)
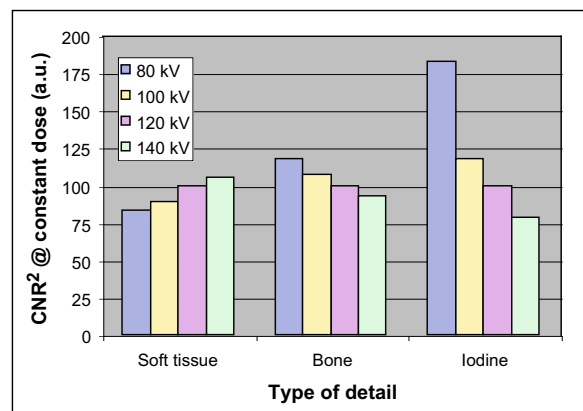

Fig. 4.29. Voltage dependence of contrast-to noise ratio squared (CNR^2) at constant patient dose ($CTDI_w$) for different types of detail. While CNR^2 is almost constant for imaging of soft tissue and bone, imaging performance is significantly improved for iodine at lower voltages

by almost a factor of two without sacrificing image quality.

Recommendation:

Tube potentials other than 120 kV should be considered only in the case of:

- Obese patients in whom mAs cannot be further increased: use higher kilovolt settings
- Slim patients and pediatric CT, where mAs cannot be further reduced: use lower kilovolt settings
- CT angiography with iodine: use lower kilovolt settings

Variations in tube potential should not be considered for pure dose reduction purposes except in the case of CT angiography. Due to the complexity involved, adaptation of mAs settings should not be left to AEC systems, as these do not account for changes in contrast. Dose settings in CT angiography should not be higher than in unenhanced scans of the same body section and should be lowered if performed at reduced kilovolt settings.

4.3.2.3
Slice Collimation (h_{col}) and Slice Thickness (h_{rec})

With single-slice CT (SSCT), the slice collimation h_{col} used for data acquisition and the reconstructed slice thickness h_{rec} used for viewing purposes were identical (except for slice profile broadening in spiral scans with increased pitch, as discussed in section 4.2.6). So there was no need to distinguish

between them. With MSCT, the slice collimation (e.g., 0.75 mm) and the reconstructed slice thickness h_{rec} (e.g., 5 mm) are usually different. Frequently, the selection of the reconstructed slice thickness is made with respect to multi-planar reformatting (MPR) purposes (e.g., 1 mm), thus creating a so-called 'secondary raw data set', i.e., a stack of thin slices from which MPR slabs with larger thickness (e.g., 5 mm) can be made for viewing purposes.

The ability to acquire longer body sections with thin slices in order to achieve an almost isotropic spatial resolution is the most important achievement of multi-slice technology. As reduced slice thickness is associated with increased image noise, this may have a significant impact on patient dose as expressed by the Brooks' formula (Eq. 4.18). Therefore, it is worthwhile to treat this matter in a somewhat more detailed fashion.

A narrow slice collimation is a precondition for a narrow slice thickness, but its impact on patient dose is restricted to aspects of overbeaming and overranging only. As these show opposed dependence on beam width, as outlined in sections 4.2.3 and 4.2.8, the question arises as to the optimized beam-width settings. As demonstrated in Figure 4.30 for a typical MSCT scanner, dose performance is almost equal with beam-width settings greater than 10 mm (a), except at short scan ranges (spine, pediatrics) where a beam width of between 10 mm and 20 mm is more appropriate (b). Beam-width settings below 10 mm should be avoided due to increased overbeaming effects unless there are other important aspects to justify overriding this recommendation.

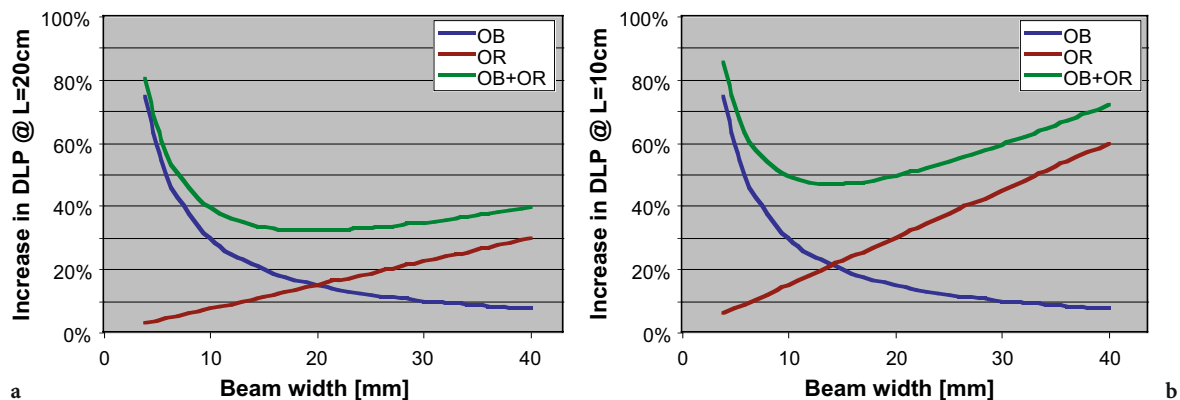**Fig. 4.30a,b.** Increased dose–length product due to overbeaming (*OB*) and overranging (*OR*) effects for a typical multi-slice computed tomography (MSCT) scanner. For average to long scan ranges (L = 20 cm and more, **a**), all beam-width settings above 10 mm perform almost equally well. For short scan ranges (L = 10 cm, as in pediatric and spine exams, **b**), beam-width settings between 10 mm and 20 mm are preferred

The decisive determinant with respect to image noise and its implications for patient dose, however, is the slice thickness h_{rec} used for viewing purposes. The relationship among slice thickness, noise and dose expressed in the Brooks' formula attempts to correct any reduction in slice thickness by a corresponding increase in dose to ensure a constant image noise, and some AEC systems exactly do so. However, any variation in slice thickness also affects image contrast due to a modification in partial volume effect, which is not taken into account by the Brooks' formula. As shown in Figure 4.31, image noise and image contrast of small details will react in a different fashion on reduction of the slice thickness: while image quality in terms of noise is impaired proportionally to the square root of the change in slice thickness only, the contrast is improved in proportion to the slice thickness. As a result, there is a net gain in image quality in terms of CNR without any increase in dose whenever partial volume effect is of importance.

This is clearly demonstrated by the clinical example given in Figure 4.32, where the visibility of a liver lesion (approximately 3 mm in size) diminishes continually with increasing slice thickness, despite reduced image noise. In addition, a detailed analysis of the results of the German survey on CT practice in 1999 (GALANSKI et al. 2001) has revealed that slice thickness has only minor or no influence on clinical dose settings. This is shown in Figure 4.33 for liver examinations with slice thicknesses of between 3 mm and 10 mm that were used in practice. Therefore, it is essential to understand that the selection
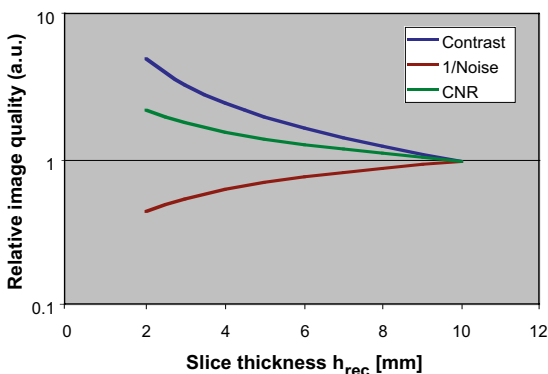

Fig. 4.31. Dependence of relative image quality on the slice thickness h_{rec}. Improvements in image quality (better detail contrast due to reduced partial volume effects) outweigh the deterioration caused by increased noise. As a result there is a net gain in contrast-to-noise ratio (CNR) at reduced slice thickness without any increase in dose

of a narrow slice collimation is only a means to an end: to enable MPR images without or with reduced step artifacts, and, if necessary, to overcome partial volume effects.

Recommendation:

The slice collimation should be selected as small as compatible with aspects of overbeaming/overranging, total scan time and tube power. Viewing should preferentially be made with thicker slabs (e.g., 3–8 mm), thereby reducing image noise and other artifacts. Thinner slabs should only be used if partial volume effect is of importance. This should preferentially be done in conjunction with workstations that allow one to change the slab thickness in real-time. Except for very narrow slices, there should be no need for any increase in dose settings on reduction of slice thickness.

4.3.2.4
Pitch (p)

With SSCT scanners, scanning at increased pitch settings primarily serves to increase the speed of data acquisition. As a side effect, however, patient dose is reduced accordingly, at the expense of impaired slice profile width, i.e., z-resolution. As already outlined in section 4.2.6, MSCT scanners make use of a spiral interpolation scheme that is different from SSCT. Thus, the slice profile width remains unaffected from changes in pitch settings. Instead, image noise changes with pitch (Fig. 4.34a) unless the tube current is adapted accordingly.

Scanners that make use of the effective mAs (mAs per slice) concept not only keep slice profile width, but also image noise constant when pitch changes (Fig. 4.34a). To achieve this goal, the electrical mAs product supplied to the X-ray tube automatically changes linearly with pitch (Fig. 4.34b). As a consequence, patient dose ($CTDI_{vol}$) is no longer reduced at increased pitch settings in contrast with SSCT scanners; neither will dose increase at reduced pitch settings. MSCT scanners without automatic adaptation of mAs will still save dose at increased pitch setting, but this will happen at impaired image quality (more noise) as long as mAs is not adapted manually.

Frequently, image quality in terms of artifacts depends on pitch settings. In general, spiral artifacts are reduced at lower pitch settings. For similar reasons, some scanners allow the setting of a limited
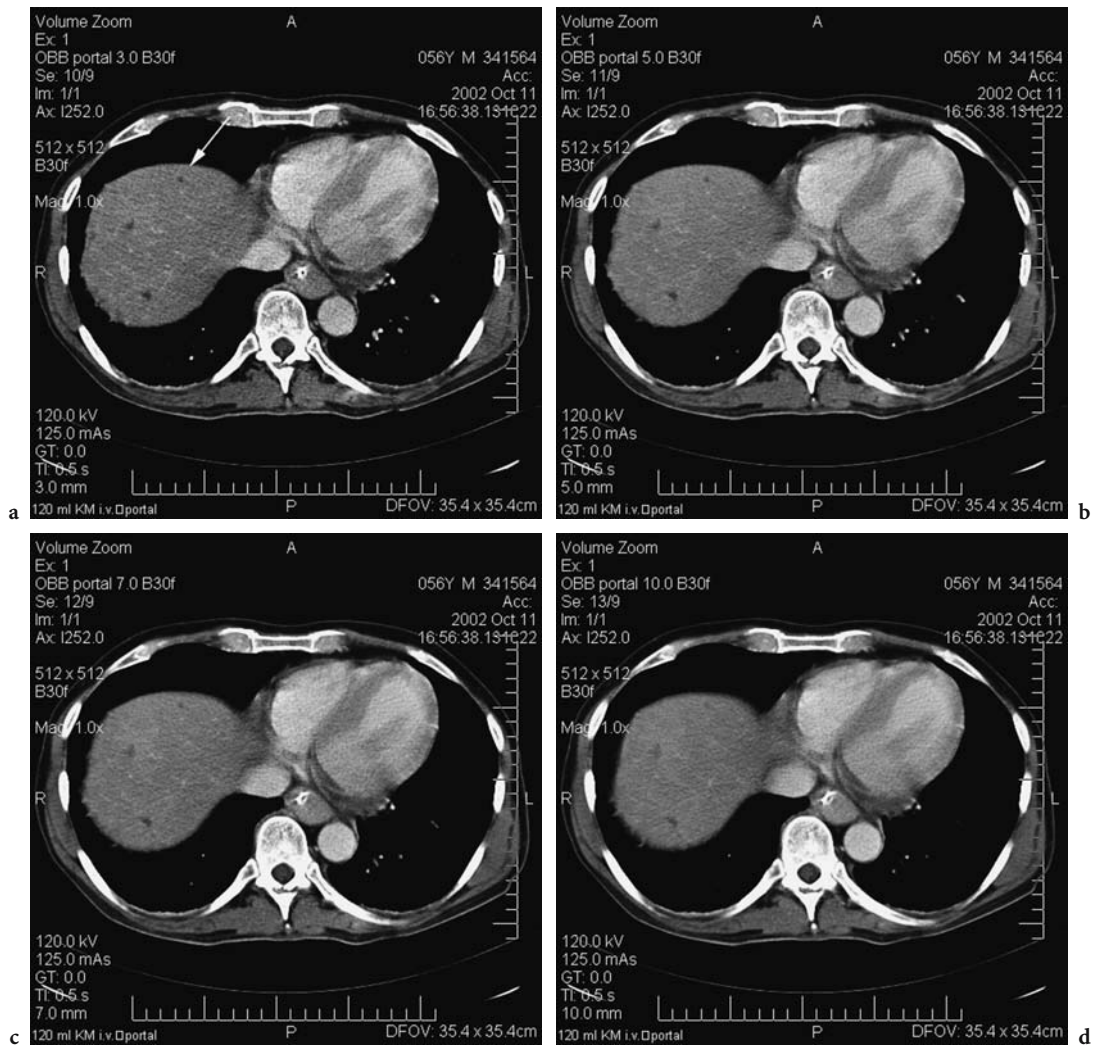
Fig. 4.32a–d. Multi-slice computed tomography (MSCT) examination of the liver performed on a MSCT scanner (Siemens Somatom Volume Zoom) at 120 kV, 4×2.5 mm slice collimation and 125 mAs$_{eff}$ (CTDI$_{vol}$ = 11 mGy). From the same raw data set, slices of different thickness [3 mm (**a**), 5 mm (**b**), 7 mm (**c**), and 10 mm (**d**)] were reconstructed at the same central position z_0. Despite the increased noise pertaining to thinner slices, the visibility of small lesions improves remarkably owing to reduced partial volume effects. This is clearly demonstrated by a lesion approximately 3 mm in size (*arrow*) (courtesy Dr. Wedegaertner, University Hospital Eppendorf, Hamburg, Germany)
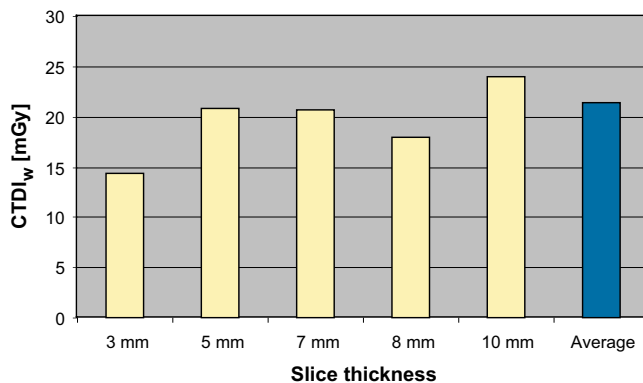

Fig. 4.33. The patient dose (CTDI$_w$) applied by the participants of the German CT survey, 1999, for liver examinations was almost constant despite the selection of different slice thickness
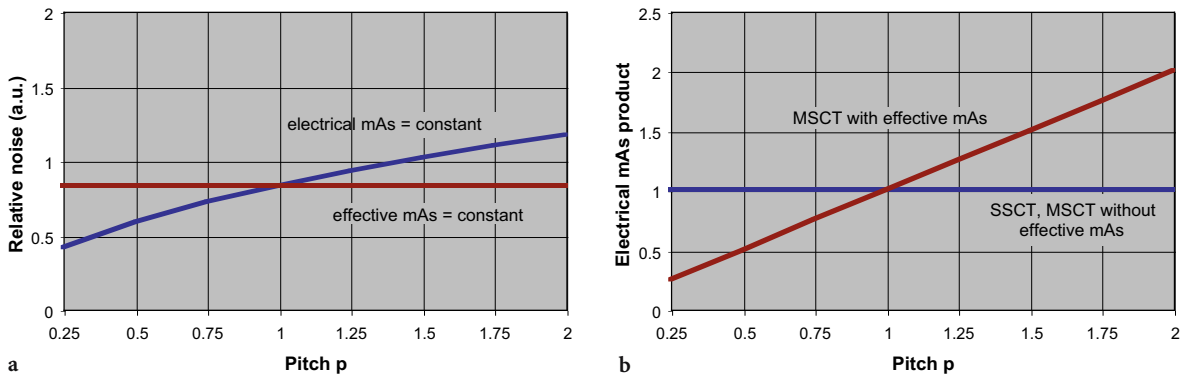
Fig. 4.34a,b. For multi-slice computed tomography (MSCT) systems that employ multi-point spiral data interpolation (z-filtering), image noise changes with pitch unless the effective current–time product (mAs$_{eff}$) is held constant (**a**). This implies that the electrical current–time product (mAs$_{el}$) supplied to the tube changes with pitch (**b**). Contrary to single-slice computed tomography (SSCT), changes in pitch settings therefore no longer have any influence on patient dose in terms of CTDI$_{vol}$

number of 'preferred' pitches only. Reduced pitch settings can also be applied to enhance the effective tube power, however, at the expense of reduced scanning speed.

Recommendation:

Pitch settings with MSCT scanners should be made exclusively with respect to scan speed, spiral artifacts and tube power. Dose considerations no longer play a role if scanners that employ effective mAs are used or if (electrical) mAs is adapted to pitch to achieve constant image noise.

4.3.2.5
Object Diameter (d) or Patient Weight (m)

Patient size, although not a parameter to be selected at the scanner's console, represents an important influencing parameter that needs to be considered in this context. Considerable reductions in mAs settings are appropriate whenever slim patients, and particularly children, are examined. In order to avoid unnecessary over-exposure, the mAs must be intentionally adapted by the operator unless AEC-like devices are available. Due to the decreased attenuation for the smaller object, image quality will not be impaired if mAs is selected appropriately. This means that the image quality will be at least as good as for patients of normal size, although the dose has been reduced.

The two questions to be solved in this context are:
- To which degree shall mAs settings be adapted in dependence of the object diameter d?

- Which diameter is typical for a standard patient to whom the standard protocol settings refer to?

From theoretical considerations (half-value thickness for CT beam qualities), mAs should be altered by a factor of two for each change in patient diameter of 4 cm tissue-equivalent thickness. However, dedicated studies (WILTING et al. 2001) have shown that this algorithm does not work well in practice: although objective (i.e., measured) noise was almost constant for patient diameters of between 24 cm and 36 cm, it was found that the subjective (i.e., perceived) image quality continually decreased with the patient diameter and vice versa. This is most likely due to the circumstance that adipose patients have more fatty tissue around their organs. Thus, the inherent contrast is better, and more noise can be tolerated. The opposite holds true with slim patients.

Consequently, a more gentle adaptation of mAs with patient diameter (factor of two in mAs per 8-cm change in patient diameter) will better comply with clinical needs. Among the AEC systems currently in use, those from Philips and Siemens already make use of this modified algorithm that ensures a constant 'adequate' image quality, while those implemented by General Electric and Toshiba simply attempt to ensure a constant noise level. As already outlined in sections 4.3.2.2 for tube potential and 4.3.2.3 for slice thickness, strategies for automatic dose control that do not account for image contrast will fall short with respect to clinical needs. Similar considerations apply to the longitudinal dose modulation functionality: in

examinations comprising several consecutive body sections with differing attenuation properties (e.g., in tumor staging of chest, abdomen and pelvis in a single spiral acquisition), mAs adjustment is often made in a way that ensures constant image noise, thus producing the highest settings in the pelvis region. However, inherent contrast in the pelvis region is much better than in the upper abdomen; consequently, reduced mAs settings would be more appropriate, as recommended in ICRP publication 88 (ICRP 2001).

Although not specified explicitly, standard protocol settings implemented by the manufacturers are usually tailored to satisfy the vast majority of clinical situations except for obese patients in whom higher mAs or kilovolt settings must be applied. So, there is good reason to refer these standard settings to patients of about 80–85 kg body weight, which is also the average weight of European males. This corresponds to a lateral diameter of 33 cm, according to a detailed analysis of patient data from a large children's hospital in Germany (SCHNEIDER 2003; Fig. 4.35a.). The following formula can be used to convert from lateral patient diameter d_{lat} (in cm) to patient weight m (in kg) and vice versa:

$$d_{lat} = 6.5 + 3 \cdot \sqrt{m} \qquad (4.19)$$

In current literature, numerous differing recommendations can be found on how to reduce mAs settings with patient weight or diameter. In Fig. 4.35b, three examples are shown, which are representative of weak (DONELLY et al. 2001), moderate (ROGALLA 2004) and strong (HUDA et al. 2000) adaptations of mAs to patient weight. As indicated by the dashed lines, mAs adaptation by a factor of two per 8-cm change in patient diameter is almost perfectly met by Rogalla's recommendation, which follows a very simple relationship:

Relative mAs ∝ body weight + 5 kg (4.20)

A similar relationship has been proposed by another research group (HONNEF et al. 2004). This formula can be used to create a set of standard protocols for different weight classes (e.g., 0–5 kg, 6–10 kg, 11–20 kg, 21–40 kg, 41–60 kg, 61–80 kg, etc.), which can easily be applied in daily practice.

Recommendation:

mAs settings should be adapted to patient size in a more gentle way (factor of two per 8-cm change in diameter) than predicted by theoretical considerations that only account for image noise. In addition, body regions with better inherent contrast should be scanned at reduced mAs settings. Preferentially, AEC systems that measure rather than estimate patient absorption should be used, provided that their algorithm makes use of this more gentle mAs adjustment. Failing this, manual adjustment using a set of patient-weight-adapted protocols based on Rogalla's formula (4.20) should be applied instead. For head examinations, mAs adaptation should not be made with respect to patient weight, but to patient age.
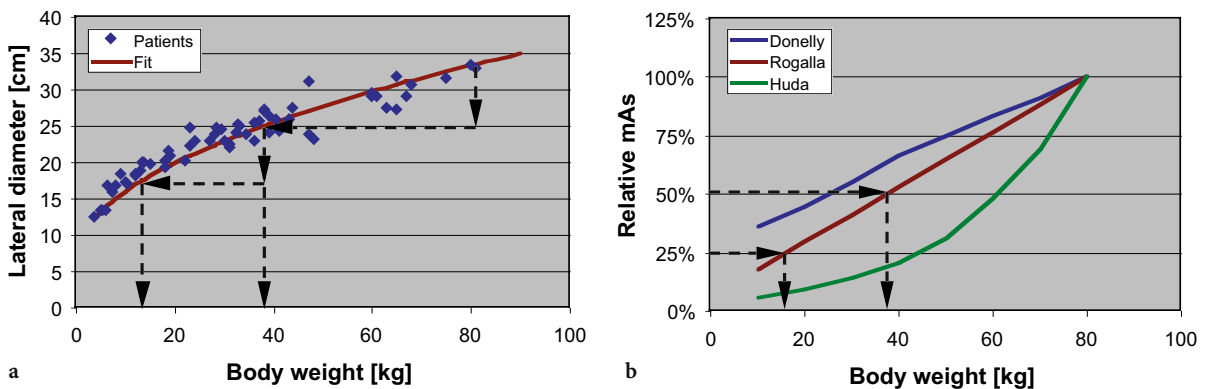
Fig. 4.35a,b. Relationship between patient weight and lateral diameter according to a detailed analysis of patient data from a big children's hospital (**a**) and dependence of patient weight on relative current–time product (mAs) settings, as recommended by three representative authors (**b**). As indicated by the *dashed lines*, adaptation of the current–time product by a factor of 2 per 8-cm change in patient diameter is almost perfectly met by Rogalla's recommendation

4.3.3
Examination Parameters

4.3.3.1
Scan Length (L)

As already pointed out in section 4.1, the local dose, i.e., CTDI, is almost independent of the length of the scanned body section. The same does not hold, however, for the integral dose quantities, i.e., DLP and effective dose. Both increase in proportion to the length of the body section. Therefore, limiting the scan length according to the clinical needs is essential.

On most scanners, the scan length, L, is usually not indicated explicitly. Instead, the positions of the first and the last slice are stated only; the same holds for the information that is documented on the images or in the DICOM data file. The net scan length, L_{net}, i.e., the length of the imaged body section, is calculated by:

$$L_{net} = \left| pos.\ first\ sl. - pos.\ last\ sl. \right| + h_{rec} \qquad (4.21)$$

while the gross scan length, L_{gross}, i.e., the length of the irradiated body section, is:

$$L_{gross} = L_{net} + \Delta L \qquad (4.22)$$

where ΔL is the increase in scan length due to over-ranging as described in Equation 4.16. As a rule of thumb that holds for the majority of MSCT scanners, the actual scan range, overranging included, is extended at each side of the planned scan range by approximately $0.75 \cdot N \cdot h_{col} + 0.5\ h_{rec}$. This amounts to approximately 2 cm for a 16-slice scanner with 20-mm beam width and 5-mm slice thickness.

Recommendation:

For each patient, the scan length should be selected individually, based on the scan projection radiograph that is generally made prior to scanning for the purposes of localization, and should be kept as short as necessary. Moreover, a reduction in the scan range should be considered in multi-phase examinations and follow-up studies. Whenever feasible, critical organs, such as the eye lenses or the male gonads, should be excluded from the scan range. This may be difficult for MSCT scanners that allow for large beam-width settings due to increased over-ranging effects.

4.3.3.2
Number of Scan Series (n_{Ser})

In CT terminology, a scan series is usually referred to as a series of consecutive sequential scans or one complete spiral scan. With the limited tube power available for many SSCT scanners, CT examinations of long body sections (e.g., tumor staging of the entire trunk) had to be separated into several consecutive subsections. If the same protocol settings are applied to each series, the local dose will always be the same, while the integral dose is the sum of the DLP or effective dose values of each series. So it would not make a difference whether the body section is scanned as a whole or in several shorter subsections, except for overranging effects that will increase proportionally to the number of subjections. However, mAs settings can be adapted to the particular needs of each subsection, e.g., lower settings for the chest, higher settings for the upper abdomen and reduced settings for the pelvis, as indicated in section 4.3.2.5.

If the same body section (or parts of it) is scanned more than once, this is usually denoted as 'multiphasic'. However, this not only applies to examinations with administration of contrast agents, but also to examinations where the same body section is scanned with different orientation (such as in facial bone exams) or with different slice collimation settings (e.g., chest standard plus high resolution). Although more than one scan is made at the same position, the length of each single scan of a multiphasic exam does not necessarily have to be the same. While it is meaningful to sum up the integral doses (DLP, effective dose) of each phase, this is not true for the local doses (i.e., $CTDI_{vol}$). Nevertheless, multi-phasic exams result in an increase in integral radiation exposure that is roughly proportional to the number of phases.

Recommendation:

The number of scan series (phases) should be kept as low as necessary. This holds true particularly for liver examinations, where studies with up to six different phases are sometimes recommended in literature.

4.3.3.3
Number of Rotations in Dynamic CT Studies (n)

In dynamic CT studies, e.g., in CT fluoroscopy or in perfusion studies, a multiple number of scans is

made at the same position. Therefore, it is meaningful to sum up the local doses, also. For this particular situation, the main issue is the avoidance of deterministic radiation effects. Local doses can be quite high if the scans are made with the standard dose settings used for that body region. Integral doses are normally comparable to the values encountered in standard examinations of the same region. However, with the advent of wider detector arrays, which may become even larger in future, integral dose will also be significantly increased.

The doses applied in dynamic CT studies depend on two factors: the dose, i.e., the $CTDI_w$, per rotation, and the number of rotations. As perfusion studies are regularly made with administration of contrast agents, the benefits of reduced kilovolt settings as described in section 4.3.2.2 should be used to reduce the dose settings. The number of rotations can be kept low by limiting the total length of the study, by reducing the image acquisition rate or by intermitting the procedure (in CT fluoroscopy) whenever possible.

Recommendations:

Dynamic CT studies should be made with the lowest dose settings, the most narrow beam width, the shortest length and the smallest image rate that is compatible with the clinical needs of the examination.

4.3.4
Reconstruction and Viewing Parameters

4.3.4.1
Filter Kernel (FK)

CT images are reconstructed from sets of attenuation measurements using dedicated mathematical procedures (algorithms) known as 'reconstruction filters' or 'filter kernels'. These algorithms are characterized as having quite different properties with regard to image quality: with highly resolving filter kernels, spatial resolution is improved but noise is increased. The opposite happens with smoothing kernels, which reduce noise at the expense of spatial resolution.

The properties of reconstruction filters are not subject to standardization. Therefore, kernels of equal or similar designation may vary considerably from one brand of scanner to the next. Equally,
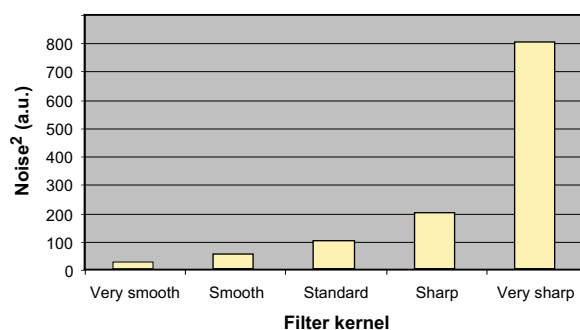

Fig. 4.36. Typical noise characteristics of different filter kernels. Relative figures are given in terms of noise squared, so the percentage differences can be translated directly into dose differences that would be necessary for constant image noise

reconstruction filters used for head or body scans carrying the same name are by no means identical. Labels such as 'smooth' or 'sharp' can only be used as coarse indicators of the balance between spatial resolution and image noise.

The compromise between spatial resolution and contrast resolution for a particular clinical indication must be found by appropriate selection of the reconstruction filter. The better the spatial resolution, the higher the noise, as indicated in Figure 4.36. Image noise, however, strongly affects contrast resolution. Due to the relationship between dose and noise given by the Brooks' formula (Eq. 4.18), the decision to use a particular filter kernel may directly affect the amount of dose required.

There are two practical sets of circumstances in which dose can be saved by proper selection of the reconstruction filter. The first is where spatial resolution is more than sufficient for a given clinical indication. Contrary to the manufacturer's recommendations, a smoother filter kernel can therefore be selected. The improvements resulting from this choice can then be used to reduce dose instead of noise, as indicated in Figure 4.37. The second is where the CNR for high-contrast structures (e.g., lungs, skeleton) is more than sufficient, even though a highly resolving filter kernel was used. In this case, increased noise can be tolerated, even if dose is reduced. So it turns out once again that the Brooks' formula is somewhat misleading as it does not account for image contrast. Nevertheless, the automatic exposure control system from one particular manufacturer also attempts to compensate for changes in noise that result from the selection of the filter kernel.

Fig. 4.37. Comparison of two images that were scanned and reconstructed with different current–time product (mAs) and filter kernel settings but result in similar image noise
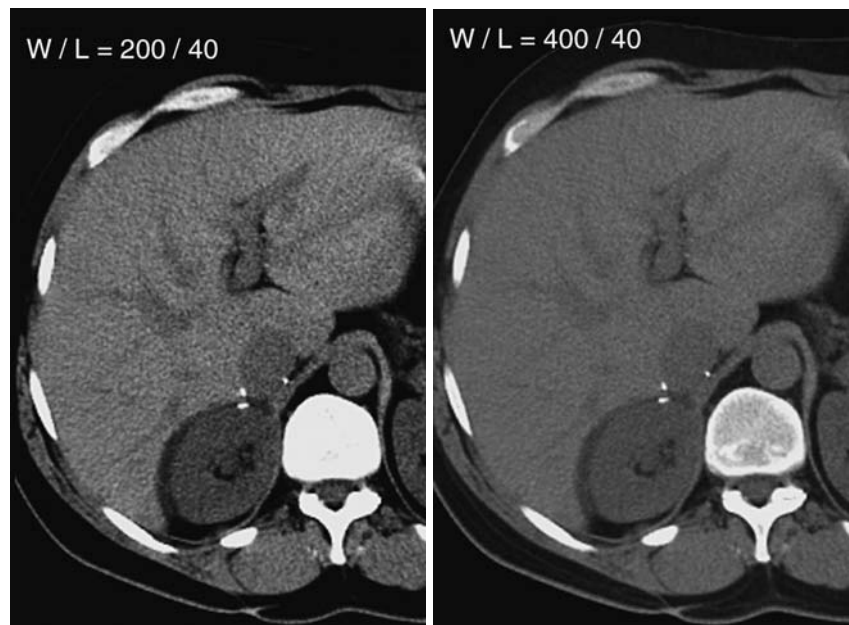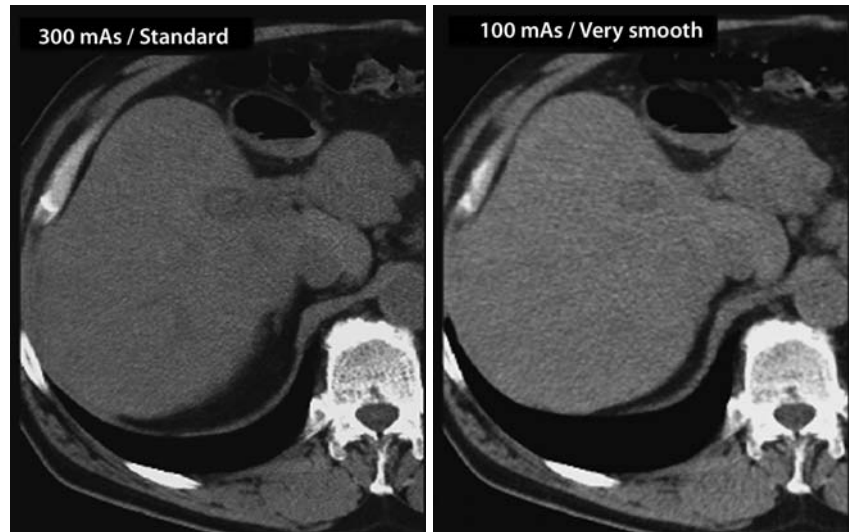

Fig. 4.38. Comparison of two images with different settings of the window width W. Wider window settings result in smoother images, thus allowing for reduced dose settings, provided that the inherent contrast is sufficiently high

Recommendation:

The selection of the filter kernel should be made with respect to the inherent contrast and as smooth as compatible with the clinical needs, thereby reducing the dose to that noise level that is appropriate. High-resolution kernels should only be used for high-contrast structures without adaptation of mAs settings.

4.3.4.2
Window Width (W)

The window width is often not regarded as a relevant factor influencing dose, since it is assumed that the width of the window is a parameter only related to image presentation. However, the visual perception of image noise strongly depends on the choice of window width setting. Using a wide window set-

ting, noise perception can be reduced, as shown in Figure 4.38. The reduction is inversely correlated to window width (PROKOP 1998). However, image contrast is also decreased, of course, because the number of gray scale values is simultaneously reduced.

Therefore, a prerequisite for dose reduction using wider window settings is the sufficiency of CNR. Due to the non-linear relationship between dose and noise, even a relatively small increase in window width is profitable: if a setting of 350 HU is used instead of 300 HU, dose can be reduced by 26% while noise perception remains the same. It is therefore worthwhile finding out whether wider settings than those recommended by the manufacturer might also be appropriate. This holds particularly for high-contrast structures; by doubling the window width, the dose can be cut to one-quarter.

Recommendation:

The window width should be selected as wide as tolerable. With high-contrast structures, the improvement in noise thus achieved should be used to reduce the dose settings.

References

Brooks RA, DiChiro G (1976) Statistical limitations in X-ray reconstructive tomography. Med. Phys. 3:237–240

Donnelly LF, Emery KH, Brody AS, Laor T, Gylys-Morin VM, Anton CG, Thomas SR, Frush DP (2001) Minimizing radiation dose for pediatric body applications of single-detector helical CT: strategies at a large children's hospital. AJR 176:303–306

European Commission (1999a) Guidance on diagnostic reference levels (DRLs) for medical exposures. Radiation Protection 109. Office for Official Publications of the European Communities, Luxembourg

European Commission (1999b) European guidelines on quality criteria for computed tomography. Report EUR 16262 EN. Office for Official Publications of the European Communities, Luxembourg, pp 69–78

Flohr T, Stierstorferr K, Raupach R, Ulzheimer S, Bruder H (2004) Performance evaluation of a 64-slice CT system with z-flying focal spot. Fortschr Roentgenstr 176:1803–1810

Galanski M, Nagel HD, Stamm G (2001) CT-Expositionspraxis in der Bundesrepublik Deutschland - Ergebnisse einer bundesweiten Umfrage im Jahre 1999. Fortschr Roentgenstr 173:R1–R66

Honnef D, Wildberger JE, Stargardt A, Hohl C, Barker M, Günther RW, Staatz G (2004) Multislice spiral CT (MSCT) in pediatric radiology: dose reduction for chest and abdomen examinations (in German). Fortschr Roentgenstr 176:1021–1030

Huda W, Scalzetti EM, Levin G (2000) Technique factors and image quality as functions of patient weight at abdominal CT. Radiology 217:430–435

ICRP (International Commission on Radiological Protection) (1991) 1990 recommendations of the ICRP. Publication 60. Pergamon Press, Oxford

ICRP (International Commission on Radiological Protection) (2001) Managing patient dose in computed tomography. Publication 88, Annals of the ICRP Vol 31, No 2. Pergamon Press, Oxford

IEC (International Electrotechnical Commission) (1999) Medical electrical equipment – Part 2: Particular requirements for the safety of X-ray equipment for computed tomography. IEC standard 60601-2-44. IEC, Geneva

IEC (International Electrotechnical Commission) (2001) Medical Electrical Equipment – Part 2: Particular requirements for the safety of X-ray equipment for computed tomography. IEC-Standard 60601-2-44 Ed. 2.0. IEC, Geneva

ImPACT (2004) Evaluation Report MHRA 04048: Sixteen slice CT scanner comparison report version 12. Medicine and Healthcare Products Regulatory Agency, London, pp 7–9

ImPACT (2005) Report 05016: CT scanner automatic exposure control systems. Medicine and Healthcare Products Regulatory Agency, London

Kalender WA (2000) Computertomographie – Grundlagen, Gerätetechnologie, Bildqualität, Anwendungen. Publicis MCD-Verlag, München, pp 127–128

Nagel HD (1986) Aluminium equivalence of materials used in diagnostic radiology and its dependence on beam quality. Phys. Med. Biol. 31:1381–1399

Nagel HD (1989) Comparison of performance characteristics of conventional and K-edge filters in general diagnostic radiology. Phys. Med. Biol. 34:1269–1287

Nagel HD (2005) Significance of overbeaming and overranging effects of single- and multi-slice CT scanners. In: Proc. 14th International Conference of Medical Physics, Nuremberg, pp 395–396

Nagel HD (ed), Galanski M, Hidajat N, Schmidt T, Maier W (2002) Radiation exposure in computed tomography – fundamentals, influencing parameters, dose assessment, optimisation, scanner data, terminology, 4th revised and updated edition. CTB-Publications, Hamburg (contact: ctb-publications@gmx.de)

Prokop M, Schäfer-Prokop CM, Galanski M (1998) Dose reduction vs. image quality in spiral CT: How far down can we go in clinical practice? In: Krestin GP, Glazer GM (eds.). Advances in CT IV. Springer Verlag, Berlin: pp 16–26

Rogalla P (2004) Personal communication

Schneider K (2004) Personal communication

Shope TB, Gagne RM, Johnson GC (1981) A method for describing the doses delivered by transmission X-ray computed tomography. Med. Phys. 8:488–495

Shrimpton PC and Wall B (2000) Reference doses for paediatric computed tomography. Radiation Protection Dosimetry 90:249–252

Stamm G, Nagel HD (2002) CT-Expo – a novel program for dose evaluation in CT (in German). Fortschr Roentgenstr 174:1570–1576

Tack D, Gevenois PA (2006) Comparison of the performance characteristics of five programs for patient dose assessment in computed tomography. Submitted to Eur. Radiol.

Taguchi K, Aradate H (1998) Algorithm for image reconstruction in multi-slice helical CT. Med. Phys. 25:550–561

van der Haar T, Klingenbeck-Regn K, Hupke R (1998) Improvement of CT performance by UFC detector technology. In: Krestin GP, Glazer GM (eds). Advances in CT IV. Springer Verlag, Berlin, pp 9–15

Vlassenbroek A (2004) Dose management in pediatric examinations. In: Proc. 2nd Philips CT user meeting, Barcelona, pp 39–44

Wilting JE, Zwartkruis A, van Leeuwen MS, Timmer J, Kamphuis AGA, Feldberg M (2001) A rational approach to dose reduction in CT: individualized scan protocols. Eur Radiol 11:2627–2632